BRL

TECHNICAL REPORT ARBRL-TR-02048

THE PHENOMENOLOGY OF INTERROUND COMMUNICATION AND TECHNIQUES FOR PREVENTION

Philip M. Howe

March 1978

USA ARMAMENT RESEARCH AND DEVELOPMENT COMMAND
USA BALLISTIC RESEARCH LABORATORY
ABERDEEN PROVING GROUND, MARYLAND

Destroy this report when it is no longer needed.
Do not return it to the originator.

Secondary distribution of this report by originating or sponsoring activity is prohibited.

Additional copies of this report may be obtained from the National Technical Information Service, U.S. Department of Commerce, Springfield, Virginia 22161.

The findings in this report are not to be construed as an official Department of the Army position, unless so designated by other authorized documents.

The use of trade names or manufacturers' names in this report does not constitute indorsement of any commercial product.

(18) SBIE (19) AD-E430 014

UNCLASSIFIED
SECURITY CLASSIFICATION OF THIS PAGE (When Data Entered)

REPORT DOCUMENTATION PAGE	READ INSTRUCTIONS BEFORE COMPLETING FORM
1. REPORT NUMBER (4) TECHNICAL REPORT ARBRL-TR-02048 — 2. GOVT ACCESSION NO.	3. RECIPIENT'S CATALOG NUMBER
4. TITLE (and Subtitle) (6) THE PHENOMENOLOGY OF INTERROUND COMMUNICATION AND TECHNIQUES FOR PREVENTION	5. TYPE OF REPORT & PERIOD COVERED (9) Final rept,
	6. PERFORMING ORG. REPORT NUMBER
7. AUTHOR(s) (10) Philip M. Howe	8. CONTRACT OR GRANT NUMBER(s)
9. PERFORMING ORGANIZATION NAME AND ADDRESS US Army Ballistic Research Laboratory (ATTN: DRDAR-BLT) Aberdeen Proving Ground, MD 21005	10. PROGRAM ELEMENT, PROJECT, TASK AREA & WORK UNIT NUMBERS (6) RDT&E 1L662618AH80, 1X664626DG24
11. CONTROLLING OFFICE NAME AND ADDRESS US Army Armament Research and Development Command US Army Ballistic Research Laboratory (ATTN: DRDAR-BL) Aberdeen Proving Ground, MD 21005	12. REPORT DATE (11) MAR 78 (12) 74 pp
	13. NUMBER OF PAGES 76
14. MONITORING AGENCY NAME & ADDRESS(if different from Controlling Office)	15. SECURITY CLASS. (of this report) UNCLASSIFIED
	15a. DECLASSIFICATION/DOWNGRADING SCHEDULE

16. DISTRIBUTION STATEMENT (of this Report)

Approved for public release; distribution unlimited.

17. DISTRIBUTION STATEMENT (of the abstract entered in Block 20, if different from Report)

18. SUPPLEMENTARY NOTES

19. KEY WORDS (Continue on reverse side if necessary and identify by block number)

Munitions interactions
Explosives sensitivity
Warhead fratricide
Explosions
Detonations

20. ABSTRACT (Continue on reverse side if necessary and identify by block number) (mba)

Examination of large scale munitions propagation tests indicated that the mechanisms by which detonation and violent reaction propagate between munitions and through stacks are inadequately understood. Experimental data were obtained with respect to interround propagation and with respect to munition response to fragment impact and deformation. The data are consistent with the assumption that ignition is caused by individual fragment impacts creating a stress level in the explosive which exceeds some critical value. The violence of the post

(continued)

DD FORM 1 JAN 73 1473 EDITION OF 1 NOV 65 IS OBSOLETE

UNCLASSIFIED
SECURITY CLASSIFICATION OF THIS PAGE (When Data Entered)

393 471

(Item 20 Continued)

ignition reaction was found to be proportional to the delivered areal impulse density, and is consistent with assuming that the reaction violence is proportional to the deformation of the explosive. Since the yield strength of the explosive is far less than that of the casing, the warhead casing essentially controls the violence of reaction.

Experiments with various shield materials and configurations demonstrated the feasibility of preventing mass detonation of contiguous stores. Low shock impedance materials were shown to be effective shields. The author presents evidence to indicate that the low impedance materials retard ignition and casing failure by reducing delivered stress levels.

TABLE OF CONTENTS

LIST OF ILLUSTRATIONS

LIST OF ILLUSTRATIONS

LIST OF TABLES

I. INTRODUCTION

Mass detonation of explosives stores is of considerable concern in handling, transportation, storage, and battlefield use of munitions. We have undertaken studies to understand the mechanisms of mass detonation and to develop techniques for reducing the severity of the phenomenon. The results of our efforts in these areas are the subject of this report.

II. BACKGROUND

In November, 1973 the Ammunition Equipment Office of Tooele Army Depot published a report on a series of tests they conducted for the Department of Defense Explosive Safety Board[1]. These tests were designed to determine the effectiveness of reducing or preventing propagation of mass detonation between class 7 stores by interspersing them with class 5 (or lower) stores. The class 7 stores are defined to be "mass detonating"[2]. Examples are the Army 155mm, 175mm 8-inch shell, M-15 mines, and the Navy's 250 lb, 500 lb, 1000 lb and 2000 lb bombs. Class 5 stores (and lower) are not considered to be "mass detonating". Examples are small arms ammunition, 90mm cartridges, bagged propellant, etc. Twenty tests were conducted; nineteen main tests and one calibration test. Tests ranged in size from a preparatory test involving 8 boxes of 90mm cartridges stacked in the open to the final test involving 33 milvan containers filled with a total of 143,764 kg (316,947 lb) of explosives (unless otherwise noted, propellant weights will be included with the explosives. Thus, in the test alluded to above, 23,875 kg (52,635 lb) of the 143,764 kg (316,947 lb) total were propellant). The first eight tests were essentially preparatory tests used in the design of the test sequence, and no further attention will be given to them here. The remaining twelve tests will be examined with some detail, as considerable insight can be gained from them, in spite of ambiguity introduced as a result of the test design.

Tests #9 through #20 were conducted in the following way. Several milvan containers were stuffed with various types of munitions and placed below ground level in the same configuration as might be encountered in a container ship. (A milvan is a trailer type container with dimensions 2.4m x 2.4m x 6.1m (8' x 8' x 20'). In containerized munitions shipments, the milvan was planned to be the smallest non-reducible unit. The decision to rely upon the merchant container reservoir in time of mobilization has made the milvan sized unit somewhat academic). One or more of the milvans (hereafter referred to as the donor) was initiated by detonating one or two of the munitions

---

[1] *Parkinson, A., and Smith, K., "T-205 Milvan Container Storage Tests," Final Report, Nov. 1973, Tooele Army Depot.*

[2] *"Ammunition and Explosives Standards," TM 9-1300-206, DA 1973.*

within it. The rest of the containers were filled with class 5 stores (buffer containers) or class 7 stores (acceptor containers). The buffer containers were placed between the donors and acceptors. Earth was not emplaced upon the tops of the test containers nor between the containers. A schematic of a typical test configuration is shown in Figure 1. Ground shock, air shock and crater volume measurements were made on each test. Data are tabulated in Table I.

Various criteria can be used to determine the effectiveness of the buffers. The distance of a specified blast overpressure versus the mass of explosive in the test should be an effective criterion, as reduction of blast was one of the primary reasons for conducting the T-205 tests. Figure 2 shows the mass of the explosive contained in each test versus the distance at which a 8.3 kPa (1.2 psi) overpressure was measured. The 8.3 kPa (1.2 psi) value was chosen because that was the pressure level reported in the T-205 test report. Reference 3 may be consulted if it is desired to derive damage radii for other levels of damage.

The solid line in Figure 2 is a reference line derived by using Hopkinson-Cranz scaling with test #20 as a reference point for a mass detonating source.* This reference line gives the values of distance (for the 8.3 kPa (1.2 psi) level) which would be obtained if the entire amount of explosive in each test were to detonate en masse; test data which deviate from this line did not detonate en masse. By dropping along the vertical to the solid line from any test point, one can find the amount of explosive in any test which contributed to the airblast. One should be very careful in inferring a buffer effectiveness from these data: test #17 had no buffering!

The test data are replotted in Figure 3. In this case, the ordinate expresses the weight of explosive contained in the donor charge only, rather than the entire explosive weight in the test. The solid curve then describes the distance at which a 8.3 kPa overpressure would be measured if the donor charge, and the donor charge only, detonated in a manner which contributed to the airblast. In all tests except #17, the yield was greater than that expected for the donor alone; the buffer and acceptor clearly participated in the event. Test #17 had no buffer and evidently not all of the explosive detonated.

[3] *Engineering Design Handbook, "Explosions in Air, Part One," AMCP AMCT-706-181 (1974).*

**Test #20 was a calibration test with one milvan loaded with 72 500 lb bombs. It did not detonate en masse upon initiation of the first bomb. After detonation of the first bomb, there were nine additional detonations involving one or two bombs each. The final detonation occurred approximately thirty minutes after the initial detonation. The final detonation blast record is used here as the reference point. Note that most of the HE participated in the last event, thus permitting its usage as a crude standard.*

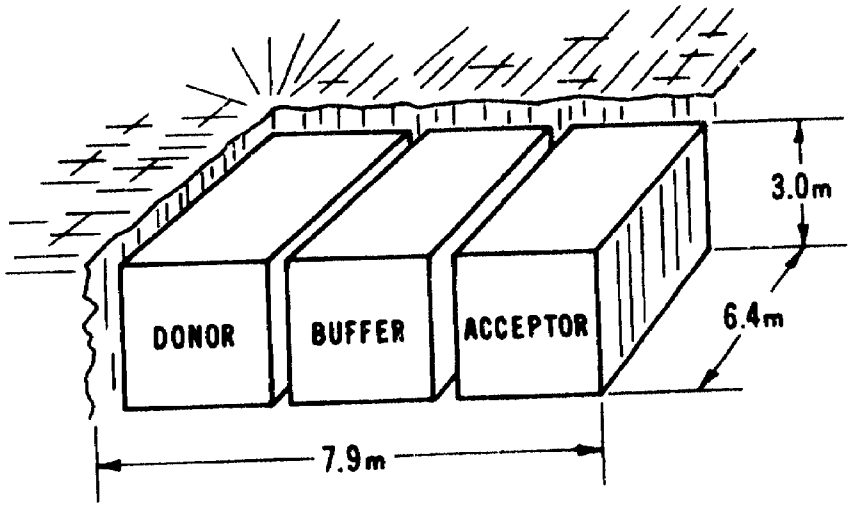

Figure 1. Schematic of Typical Test Configuration in Tooele Test 1-205

Table 1. Compilation of Data from T-205

Test No.	Donor (Kg HE)	Buffer (Kg HE)	Acceptor (Kg HE)	Total HE (Kg)	Distance for 1.2 psi overpressure (m)	Crater Volume (m x m x m)	Rounds Recovered
9	384 M15 mines (3962.65)	600 90mm cartridge (2574.63)	384 M15 mines (3962.65)	10499.93	304.80	31.1 x 29.3 x 6.1	36 90mm
10	384 M15 mines (3962.65)	1200 90mm cartridge (5149.27)	384 M15 mines (3962.65)	13074.57	243.84	25.9 x 30.8 x 5.9	241 mines 322 90mm
11	384 M15 mines (3962.65)	1080 155mm prop charges (15480.46)	384 M15 mines (3962.65)	23405.76	381.00	38.4 x 38.4 x 7.8	None
12	384 M15 mines (3962.65)	100,800 .50 cal cartridge (1534.98)	384 M15 mines (3962.65)	9460.28	228.60	27.7 x 27.7 x 4.1	246 mines many .50 caliber cartridge
13	72 500 lb bomb (6270.57)	1200 90mm cartridge (5149.27)	384 M15 mines (3962.65)	15382.48	335.28	37.8 x 37.8 x 5.8	36 90mm
14	72 500 lb bomb (6270.57)	1200 90mm cartridge (5149.27)	72 500 lb bomb (6270.57)	17690.40	289.56	20.1 x 20.1 x 7.8	292 90mm cartridge 60 500 lb bomb
15	144 500 lb bomb (12541.13)	1200 90mm cartridge (5149.27)	72 500 lb bomb (6270.57)	23960.97	335.28	33.8 x 33.8 x 7.6	505 90mm cartridge 82 500 lb bomb
16	72 500 lb bomb (6270.57)	600 90mm cartridge (2574.63)	72 500 lb bomb (6270.57)	15115.77	268.76	31.7 x 31.7 x 7.6	72 90mm cartridge 22 bombs
17	72 500 lb bomb (6270.57)	-	-	6270.57	220.98	29.9 x 29.9 x 4.3	-
18	72 500 lb bomb (6270.57)	960 90mm cartridge (4119.60)	72 500 lb bomb (16660.73)	16660.73	283.46	31.1 x 31.1 x 5.9	257 90mm cartridge 67 bombs
19	144 500 lb bomb (12541.13)	7200 90mm cartridge (30896.96)	1152 500 lb bomb (100329.06)	[illegible]	701.04	-	1 bomb 5 90mm cartridge
20	72 500 lb bomb (6270.57)	-	-	6270.57	262.13	34.1 x 34.1 x 21.3	2 bombs

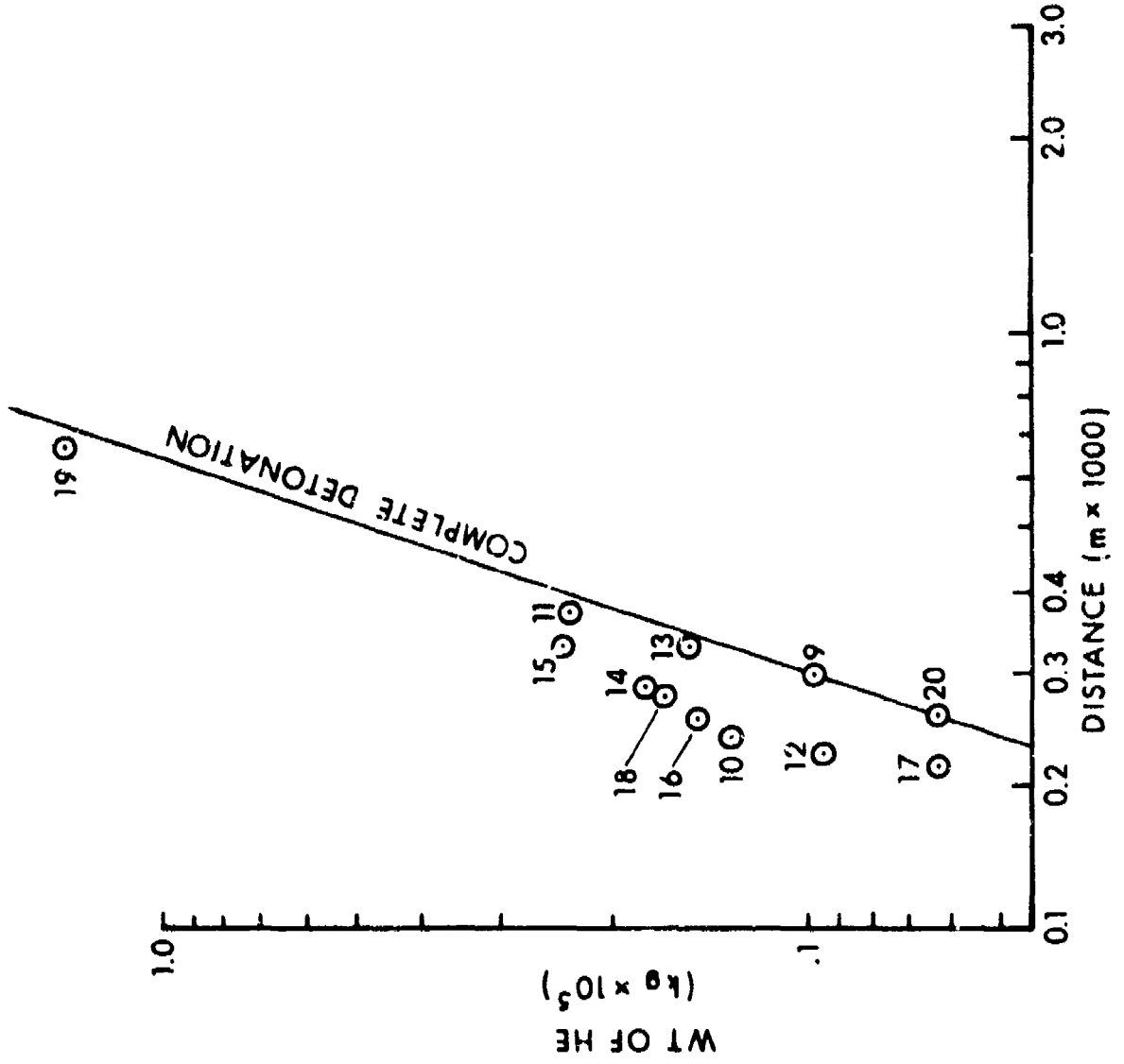

Figure 2. Mass of Explosive in Each Test Versus Distance at Which a 1.2 psi Overpressure was Recorded

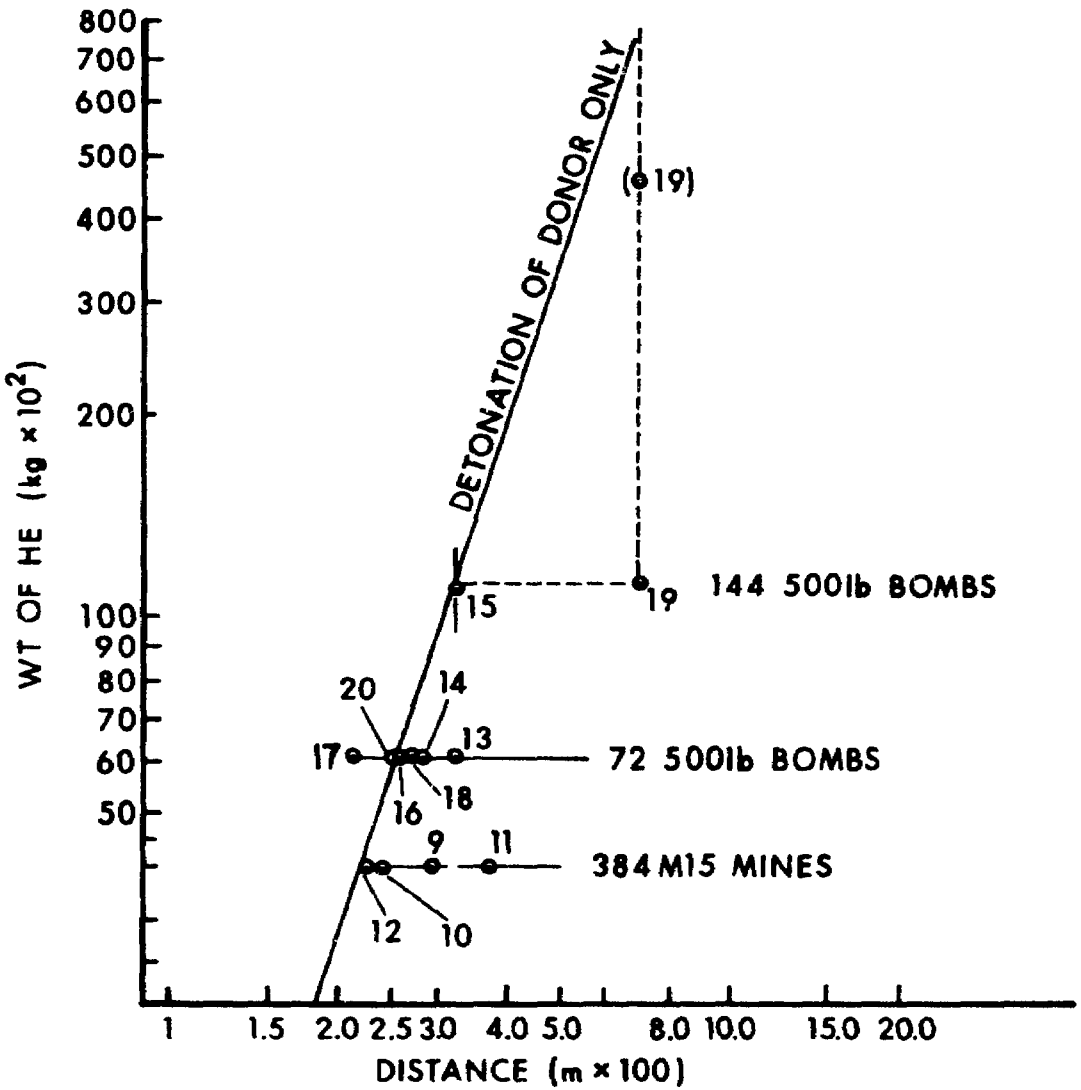

Figure 5. Mass of Explosive in Donor Charge Versus Distance at Which 1.2 psi Overpressure was Recorded

Two points are plotted for test #19, which was the largest test in the series and was the "proof of the pudding". The test layout is shown in Figure 4. In the T-205 final report, it is stated that test #19 had two milvans of bombs serving as a donor charge. From the figure, this is clearly incorrect and we must consider the donor as composed of twelve milvans of bombs, as any acceptor next to the donor acts as part of the donor. Both values are plotted in Figure 3, with the 12-milvan donor value in parenthesis. On the basis of either value, it is unjustified to infer that the buffer vans served any useful purpose. The 8.3 kPa distance for test #19 corresponds to an explosive charge of 124738 kg (275,000 lb). The test had a total of 143,765 kg (316,947 lb), which means that 19,051 kg (42,000 lb) or 13%, did not participate. (A 13% change in yield corresponds to only a 4% change in damage radius).

The mass of explosive included in each test versus the crater volume is plotted in Figure 5. Crater volume scales as the energy of the source[4], and we should expect the data to correlate well with the blast data. In general this was the case, although there was considerably more scatter in the crater volume data. (Generally the test data falls to the left of the line because the en masse detonations do not involve 100% of the total explosive present. Reference the next paragraph.) It is felt that the crater volume data do in no way vitiate the conclusions arrived at from consideration of the airblast data.

The results of the T-205 tests permit some important and interesting conclusions. In practically every test, some munitions were recovered. While the number of recovered rounds is not a useful diagnostic*, it is important to realize that not all the munitions reacted in the test events, even under admittedly severe conditions. Thus, it may be that appropriate shielding, spacing, reconfiguring, etc will permit considerable reduction in the tendency to detonate en masse.

The buffering, as used in the T-205 tests, was inadequate. It may be that some buffering effect occurred, and careful statistical analysis of the airblast data might show this. However, the effect is too slight to be important. Above the container level, with containers using existing stuffing and packaging procedures, there appears to be no easy way of generating an acceptably safe container stacking configuration without going to prohibitively large container separation distances. If one assumes the thickness of buffer required between donor and acceptor must

---

[4] *Baker, W., Weston, P., Dodge, F., "Similarity Methods in Engineering Dynamics," Spartan-Hayden, Rochelle Park, N.J. (1973).*

**Events subsequent to the mass detonation, such as cookoff, would reduce the number of munitions recovered (this happened in test #10, for example). Partial detonation of the donor charge might increase the number of munitions recovered, giving an unrealistically high value to buffer performance (see test 15, where clearly the donor did not detonate fully).*

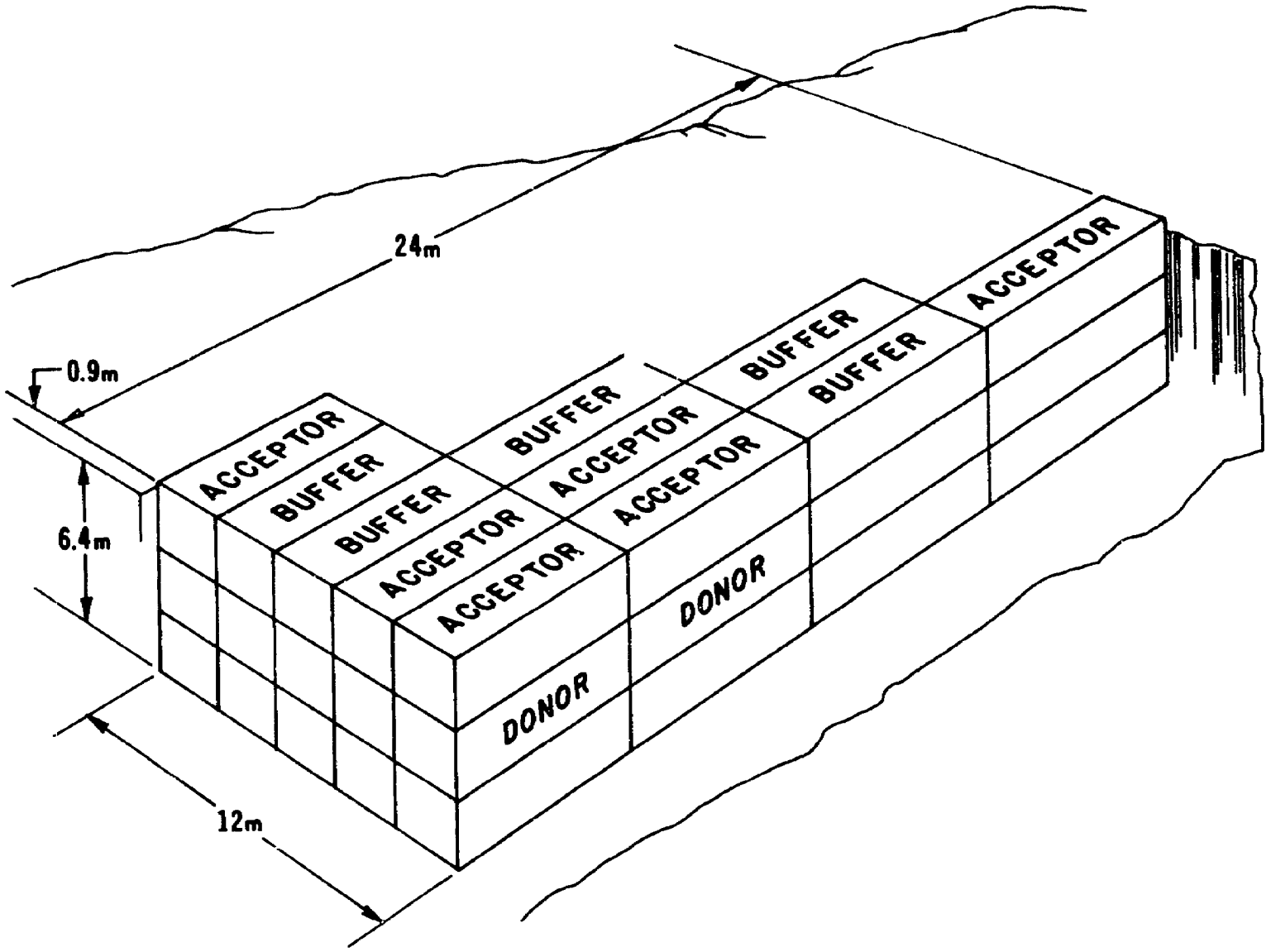

Figure 1. Schematic for Test #19 of T-205

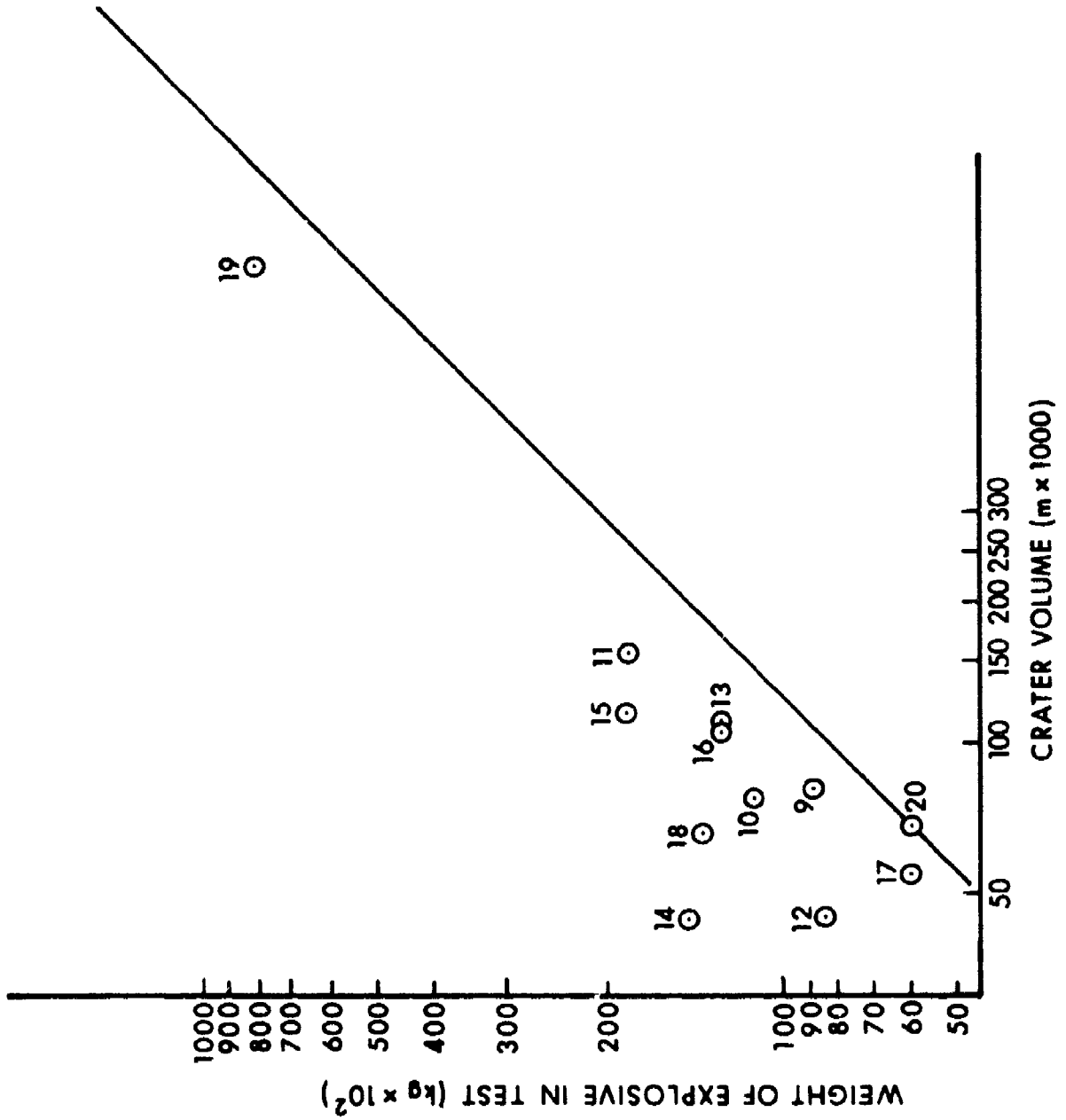

Figure 5. Mass of Explosive in Test Versus Crater Volume

be as great as the thickness of the donor, then for a donor of one munitions-filled container, seven buffer containers are required. (This is based upon assuming a rectangular array of containers, with donors and acceptors placed to exclude side, edge and corner contacts).

The use of 90mm cartridges as a buffer material has been criticized. The point was raised that, with a strong stimulus such as from the 500 lb bombs, the 90mm cartridge would react and provide a vehicle for detonation to propagate through the buffer. To check this point, we had Tooele Army Depot conduct an additional test which replicated test #9 of the T-205 with the exception that, in place of live 90mm ammunition, inert rounds (with the same total mass and area) were used as the buffer. A milvan of 384 M15 mines served as the donor charge, and another milvan of mines served as the acceptor. Two mines were used to initiate the donor charge. One hundred eighty mines were recovered, part of which may have been from the donor. Comparative data for T-205 test #9 and this test are shown in Table II. In this test, the fragment initiation mechanism was precluded both by the use of inert rounds and by staggering them in the buffer, thus fragments from the donor could not penetrate to the acceptor. Thus, the fact that fifty percent or more of the acceptor detonated clearly shows that the large scale crushing is an extremely important mechanism.

Table II. Comparison of Tests using Live and Inert 90mm Cartridges

	T-205 #9	Expl. Wt kg (lb)	Replica
Donor	384 ea M15 Mines	3963 (8736)	384 M15 Mines
Acceptor	384 ea M15 Mines	3963 (8736)	384 M15 Mines
Buffer	600 ea 90mm Cartridges	2574 (5676)	600 ea Inert 90mm Cartridges
Recovered	36 ea 90mm		180 ea M15 Mines
	0 ea M15 Mines		31 ea Inert Cartridges
Crater Size	31m x 29m x 6m (102' x 96' x 20')		29m x 27m x 5.2m (96' x 87' x 17')

A major complication introduced by the crushing mechanism is that crushing depends upon the total impulse delivered to the target, provided that a threshold pressure (the yield stress) is exceeded. The pressure and impulse delivered to a munition in a matrix, from a wave propagating through some sort of buffer material should obey Hopkinson-Cranz scaling. Thus, if one doubles the radius of the donor charge one can maintain the same peak pressure by doubling the separation distance of the acceptor from the donor. However, the impulse delivered to the

acceptor will still be twice as great. Thus, protecting against crushing as a propagation mechanism becomes prohibitively difficult as donor charge size is increased. Furthermore, the crushing of explosives can lead to ignition and buildup to detonation at very low stress levels, compared with those required for shock initiation.

The conclusion that the maximum acceptable donor charge is smaller than that containable in a standard container, coupled with the constraint that the smallest logistical unit be a container, requires that measures be taken to insure that detonation cannot propagate through a container. For this reason we have pursued investigations of the mechanisms of round-to-round propagation and techniques for reducing the probability of round-to-round propagation.

III. MECHANISMS OF INTERROUND COMMUNICATION

The detonation of a munition within an array as encountered in palletized or containerized stores creates an environment which includes fragments with a wide range of masses and velocities, and blast loading* with peak pressures and impulses (which at a given distance from the source are strong functions of donor charge mass). Thermal loads typically persist for milliseconds if only the donor charge participates, but can last for orders of magnitude longer if pallet material and other fire sources participate. Detonation and violent reaction can propagate as a result of any of the above stimuli. Both fragment impact and the detonation product loading can cause detonation of the acceptor rounds in times short with respect to significant attenuation of the donor charge shock wave - hence the term "mass detonation". Propagation of detonation or violent reaction by thermal loading - "cookoff" - is much slower. Cookoff will not be addressed in this report.

A. Initiation of Violent Reaction or Detonation by Fragment Impact - The Classical Shock Initiation Regime

The impact of a steel fragment upon an explosive charge produces a response in the explosive which depends upon the nature of the explosive, the confinement or, if unconfined, the size of the charge, and various fragment characteristics. At high impact velocities which produce strong shocks within the explosive, initiation of detonation occurs by a classical shock initiation mechanism**. When fragment impact

Blast loading is used here in a generic sense. It includes the loading developed by impact of explosive products at small distances from the donor charge as well as airshock loading.

**Classical shock initiation is defined as single transit shock initiation. The impacting projectile generates a strong shock which induces reaction in the explosive sufficiently rapidly to feed energy into the shock wave. Because of the additional energy, the shock accelerates. This process can continue until steady-state detonation is reached. It is the dominant mechanism involved in tests like the large and small gap test, and flying plate experiments on bare charges.*

experiments are performed on bare charges, or charges with a cover plate, the only mode of initiation observed is classical shock initiation. This is because, when the charge fails to detonate, it breaks apart; the explosive is scattered, and the event is recorded as a non reaction.

Gittings has shown that, for PBX 9404, the duration of the input shock required for initiation is a function of the shock pressure[5]. Walker and Wasley have expressed the functional dependence in terms of a critical energy criterion[6]. The criterion states that detonation results when a critical amount of energy per unit area is delivered to the explosive. The criterion may be expressed by the equation,

$$Put = const$$

or

$$\frac{p^2 t}{\rho_o U} = const$$

where

P is the peak pressure

u is the particle velocity

t is the shock pulse width

ρ_o is the initial explosive density

U is the shock velocity in the explosive.

When U is slowly varying, the criterion may be approximated by

$$p^2 t = const.$$

Further discussion of this is given in Reference 7.

---

[5]*Gittings, E., Fourth Symposium (International) on Detonation, Sacramento, 1970.*

[6]*Walker, F., and Wasley, R., Explosivstoffe 17, 9, (1969).*

[7]*Howe, P., Frey, R., Taylor, B., and Boyle, V., Sixth Symposium (International) on Detonation, San Diego, (1976) p. 8, ff.*

Frey has shown that the critical energy criterion can be applied to fragment impact initiation of detonation in the regime where initiation occurs by the classical shock mechanism[8]. He noted that the pulse duration, t, is controlled by rarefactions reaching the shock front and used that observation to compute values of Put for Dewey and Slade's data[9]. For bare charges and charges with cover plates, t is calculated using the sound speed in the metal predicted by Jacobs' formula[10]:

$$C = \frac{(U - u)\ (U + us)}{U}$$

where C is the sound speed, and s is a Hugoniot parameter determined by fitting the curve $U = a + su$, to experimental equation-of-state data.

For right circular cylindrical projectiles impacting normally, the controlling rarefactions are centered on the periphery (for projectile length/diameter ratio greater than 0.5) of the impacting surface or (for $L/D < 0.5$) on the back surface of the projectile. Using this reasoning, Frey showed that a plot of $\frac{1}{\sqrt{D}}$ versus threshold impact, V, velocity should be linear for $L/D > 0.5$ fragments. His approach is straightforward: Jacobs' formula predicts that the sound speed, C, varies as u. The time required for a rarefaction to reach the shock is proportional to $\frac{D}{U - C}$, or thus proportional to D/u. Since, from the conservation equations. $P = \rho_o uU$,

$$Put = \text{constant}$$

implies

$$\rho_o u^2 D = \text{constant}.$$

Since u is proportional to V, one has

$$\rho_o V^2 D = \text{constant}.$$

Dewey and Slade's data for the bare charge initiation of detonation are plotted in Figure 6. Although not apparent from this figure, the data are quite linear in the $D^{-1/2}$ versus V plane, corroborating the thinking outlined above.

---

[8]*Frey, R., Melani, G., Chawla, M., and Trimble, J., Sixth Symposium (International) on Detonation (1976) p 329 ff.*

[9]*Dewey, J., and Slade, D., BRL Report No. 1021 (1957).* (AD #145868)

[10]*Allison, F., BRL Report No. 1294 (1965).* (AD #477154)

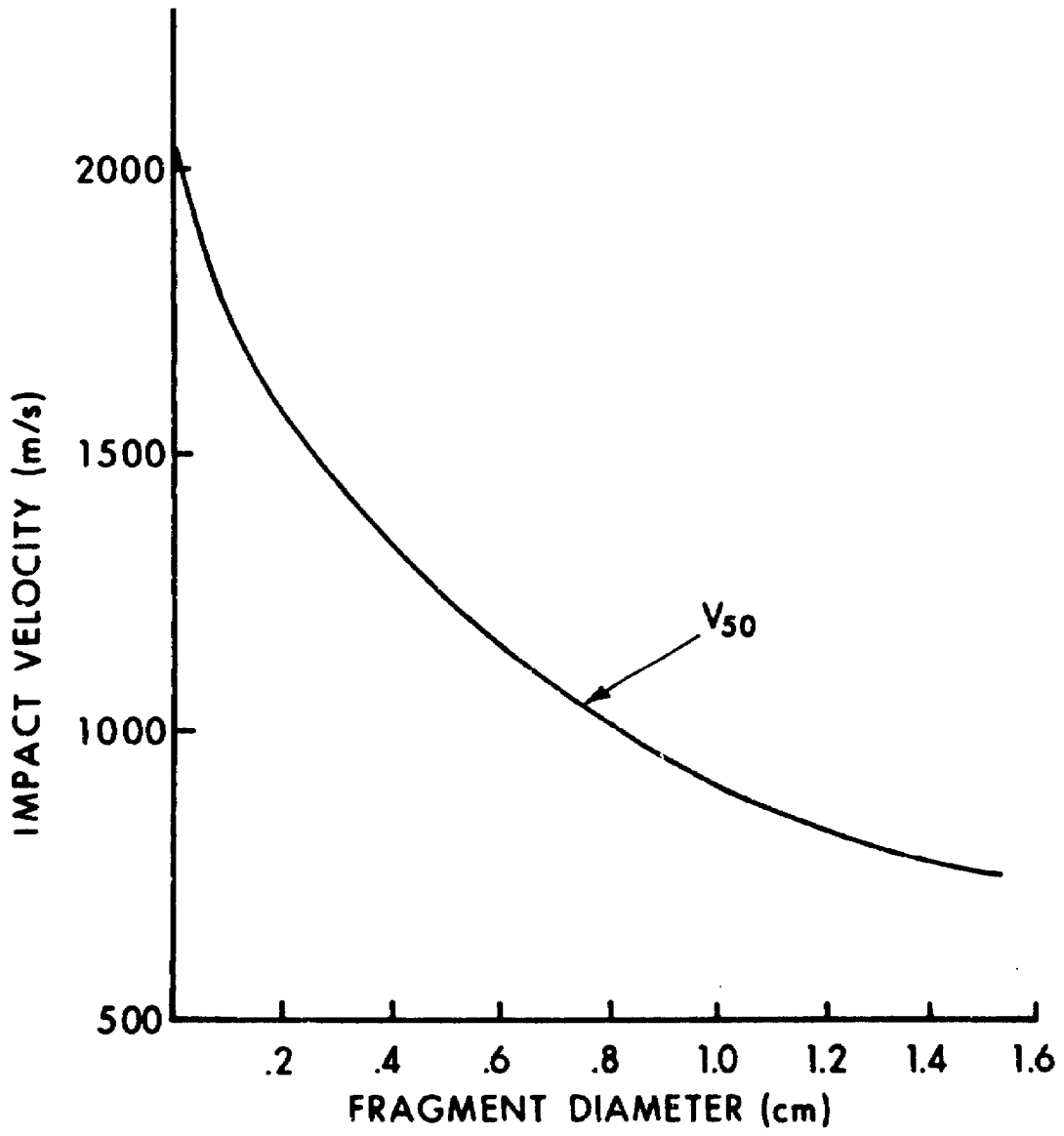

Figure 6. Dewey and Slade's Data for Fragment Impact Initiation of Unconfined Composition B

B. The Effect of Confinement

When the explosive charge is heavily confined, as it is in shell*, modes other than classical shock initiation become determinants in establishing threshold criteria. While for bare charges one normally observes either detonation or no reaction, confinement permits a continuum of responses ranging from no reaction; ignition** with subsequent extinction of burning, initiation of sustained burning, violent reaction, and detonation. The time for initiation of detonation by classical shock initiation is usually of the order of 10 μsec. The time to explosion or violent reactions which cause breakup of the casing into small fragments are usually of the order of hundreds or thousands of microseconds.

Reeves has published data on the initiation of Composition B loaded shells subjected to fragment impact[11]. His experiments used steel, right circular cylindrical fragments with L/D = 1. Impact points were just above the bourrelet which, in most shell, is the thinnest part of the casing. His data for 105mm HE shell are presented in Figure 7. He made no distinction between violent reactions and detonations.

Frey has made calculations of the mass and velocity of fragments required to initiate detonation 50% of the time[8]. He used the critical energy criterion and assumed that the pulse duration was determined by the time for rarefactions to reach the shock front. The effect of the casing was considered by correcting for the speed of sound in the steel. His predicted curve and Reeves' data are shown in Figure 8. The predicted curve is a good measure of what the detonation threshold would be if it occurred as a result of shock initiation. Note that the heavily confined Composition B is susceptible to explosive reactions under conditions where the classical shock mechanism cannot be operative.

This author has sponsored work at New Mexico Institute of Technology to extend Reeves' data on Composition B loaded 105mm shell to larger fragments[12]. The same test conditions were used, as in Reeves' work. The data, with Reeves' data, are plotted in Figure 9. Note that the data base covers nearly three orders magnitude change in mass. The data are presented in Figure 10 in the $D^{-1/2}$ versus V coordinate system.

For purposes considered here, even the Army's 105mm HEP round, which has a relatively thin skin, is "heavily confined".

**The words "ignition" and "initiation" are used quite precisely here. "Ignition" is taken to mean establishment of exothermic chemical reaction. "Initiation" is taken to mean establishment of some response beyond ignition, eg., initiation of detonation, or initiation of violent reaction.*

[11] *Reeves, H., BRL Report No. 2031 (1971).*

[12] *Collis, D., private communication.*

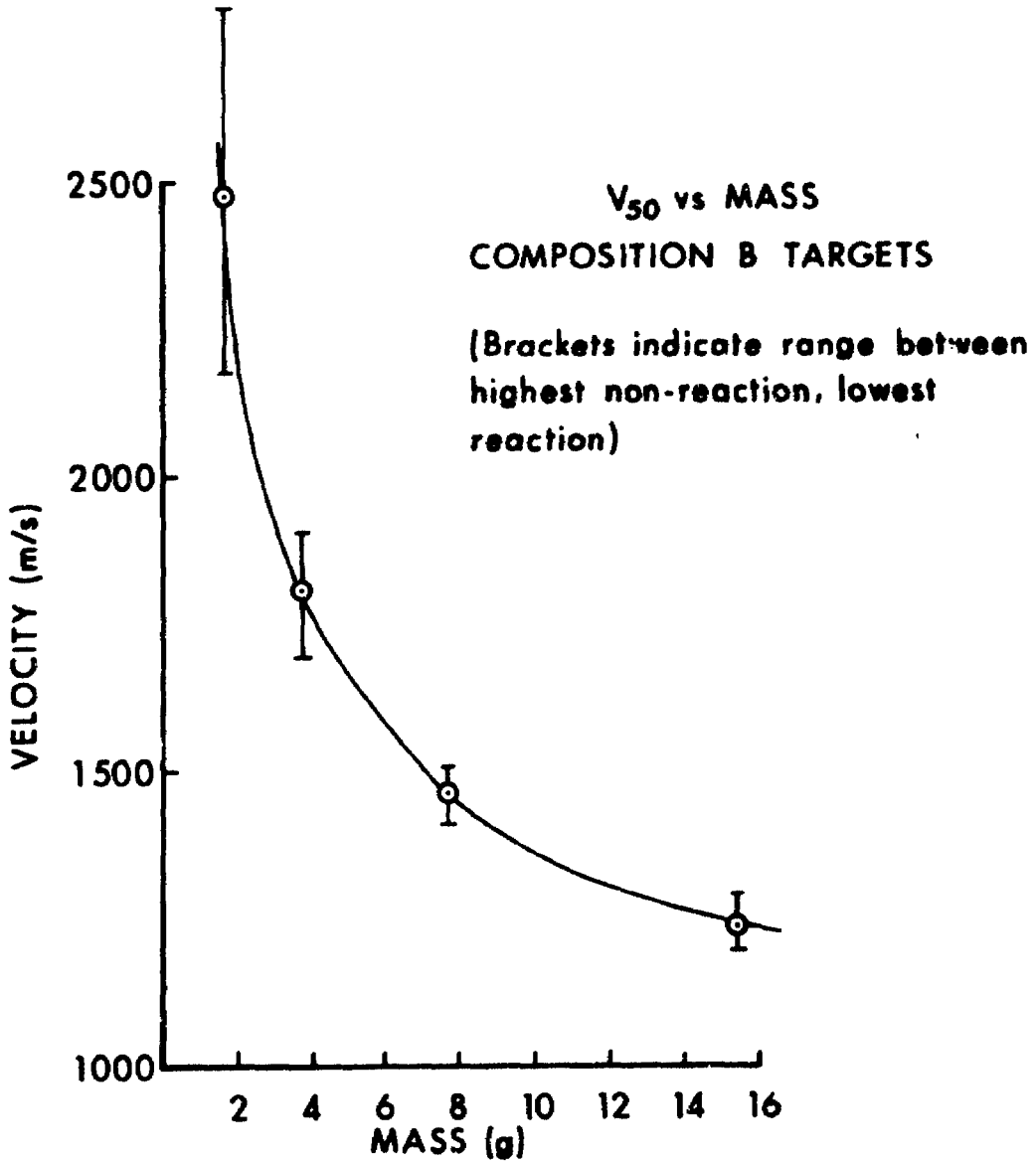

Figure 7. Reeves' Data for Fragment Impact Initiation of 105mm HE Shell

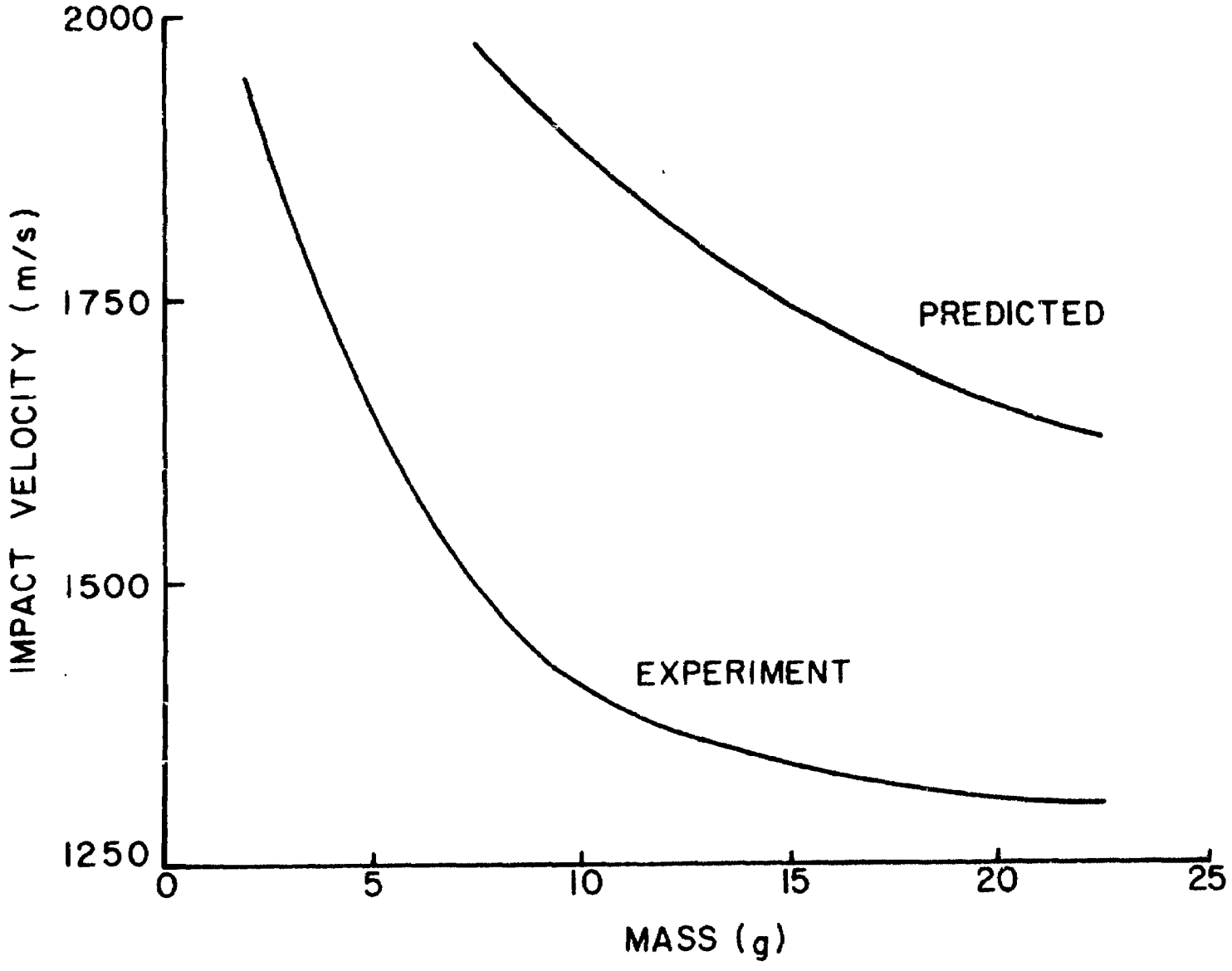

Figure 8. Comparison of Reeves' Data with Frey's Prediction, Based Upon A Shock Initiation Criterion

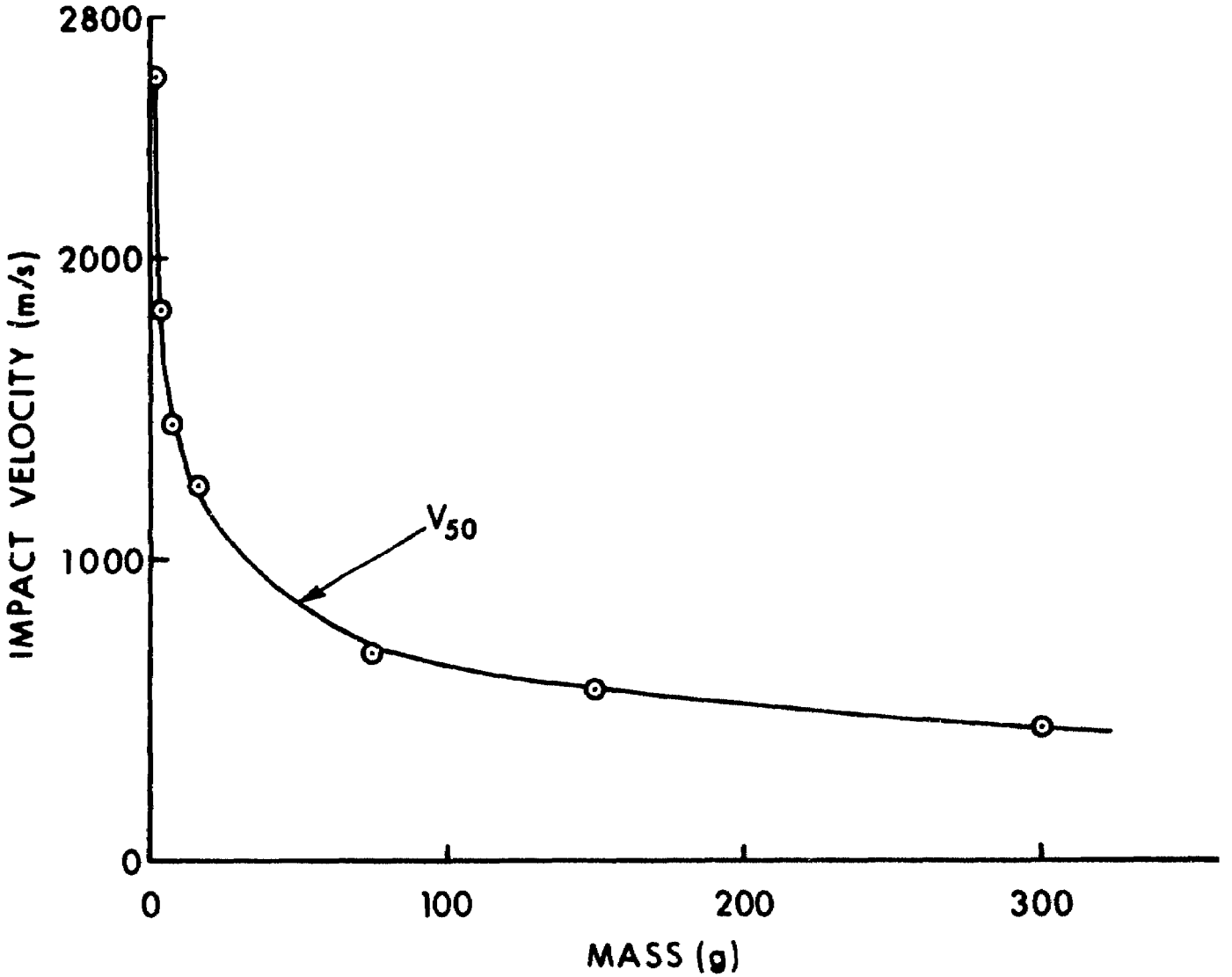

Figure 9. Compilation of Data for Fragment Impact Initiation of 105mm HE Shell

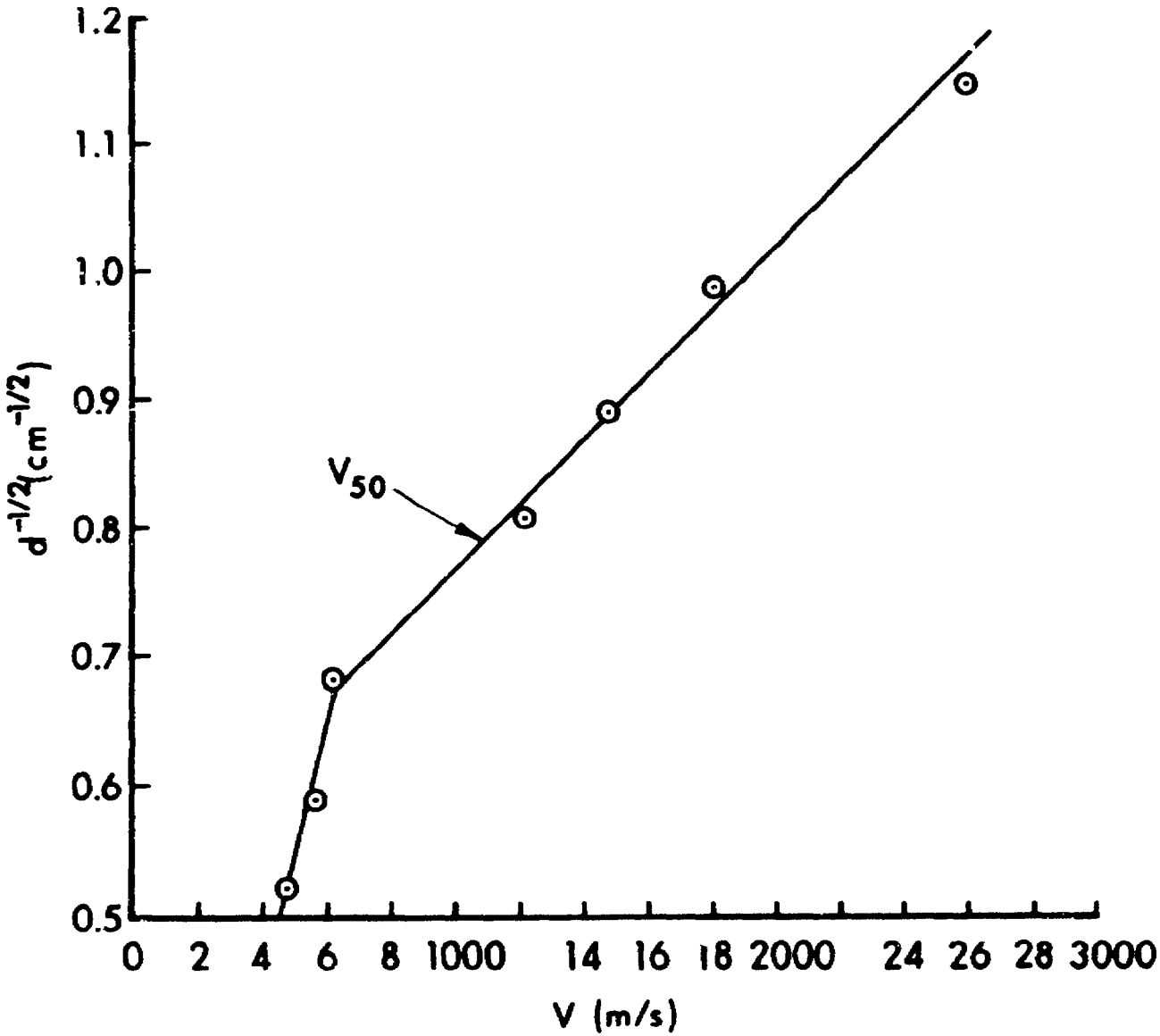

Figure 10. Data from Figure 9, Showing Inapplicability of Critical Energy Criterion

Note the non-linearity of the data in this plane, indicating that the critical energy criterion is not applicable. Published literature contains no theory which adequately explains the data. This topic will be discussed further in the next section of this report.

IV. INTERROUND COMMUNICATION

The results of several investigators provide important clues regarding the mechanism of interround communication. Afanase'ev and Bobolev have generated evidence that during impact under drop weight test conditions, the explosive fractures prior to reaction[13]. These authors suggest that ignition occurs as a result of energy released at sliding surfaces. Heavens et al., have conducted additional studies of the response of thin layers of explosive to drop weight impacts[14]. Their strain gauge measurements showed peak loading pressures of 0.5-1.0 GPa, with durations of loading 300 - 500 μsec. These authors found that the impacted explosives underwent severe plastic deformation. In all instances, ignition occurred only after plastic failure of the sample. This plastic flow takes place once the yield strength, P_y, of the layer is exceeded. The von Mises yield criterion applied to a thin layer is

$$P_y = \sigma_y \left(1 + \frac{d}{3\sqrt{3}\, w}\right)$$

where σ_y is the uniaxial tensile stress of the material, d its diameter, and w its thickness. It predicts that the greater the diameter and the smaller the thickness of the sample the greater the failure stress. Heavens[14] points out that this result is consistent with available data on the effect of sample size.

Napadensky has examined the response of unconfined explosive cylinders of several kilograms weight to large mass, low velocity impact by steel plates[15]. Her experiments were designed to subject the samples to a relatively slow crushing process; initiation of violent reaction occurred at much lower impact stress levels than required for shock initiation. Her results are not entirely consistent with those of Heavens et al. The impact velocity required to initiate violent reaction increased with increased sample length and decreased with increased diameter in her experiments.

---

[13] *Afanase'ev, G., and Bobolev, V., Daklad. Akod. Nauk SSR, 138, 886 (1961).*

[14] *Heavens, S., Field, J., Proc Royal Soc., A338, 77 (1974).*

[15] *Napadensky, H., Fourth Symposium (International) on Detonation, Sacromento (1970).*

The apparent discrepancy may be explained in the following way: In Heavens experiments, the impact velocities were quite low, and the emphasis placed by the experimental design was upon ignition. After fracture of the samples, rapid deformation occurred; but the criterion for ignition was that fracture occur. In Napadensky's experiments, the impact velocities were much higher, and fracture always occurred. Thus, ignition most likely occurred also. However, ignition without violent reaction was not observable, as the samples were always destroyed. The dependence of Napadensky's results on length and diameter of the charge can be explained by noting that the shear deformation (and rate of deformation) for a given impact velocity increases with increasing sample diameters and decreasing length[16]. If the explosive response is controlled by the degree and/or rate of deformation, this would explain the trends. (Note that the rate of reaction increases with decreased particle size in a grain burning reaction[7]. Thus, deformation and breakup of the explosive would markedly accelerate reaction. Similarly, large rates of deformation would favor formation of additional ignition sites due to frictional or viscous heating.) Whatever the details of the mechanism, it is clear that, at impact velocities of interest here, deformation of the explosive plays an important role in initiation of violent reaction.

All of the above work was conducted upon unconfined explosives. Frey has made pressure measurements in confined charges subjected to weak shock loading typical of fragment impact conditions[8]. His measurements were made in heavily confined Composition B targets. Manganin stress gages and constantan strain gages were imbedded in the explosive. A typical result is shown in Figure 11. The pressure rises slowly at first, but increases rapidly after exceeding a certain value. The time at which the pressure increases rapidly coincided with the time at which significant strain occurred. This provides additional evidence that runaway reaction occurs as a result of significant deformation. We use these conclusions and some additional assumptions to generate a simplistic model of interround communication.

All data to date indicate that the conditions for violent reaction or detonation are*

- ignition
- sufficient deformation to accelerate burning
- sufficient confinement to get a runaway reaction or explosion

---

[16] *Frey, R., private communication.*

**Classical shock initiation is excluded from consideration, as it requires much more severe loading conditions than are necessary to cause violent reaction.*

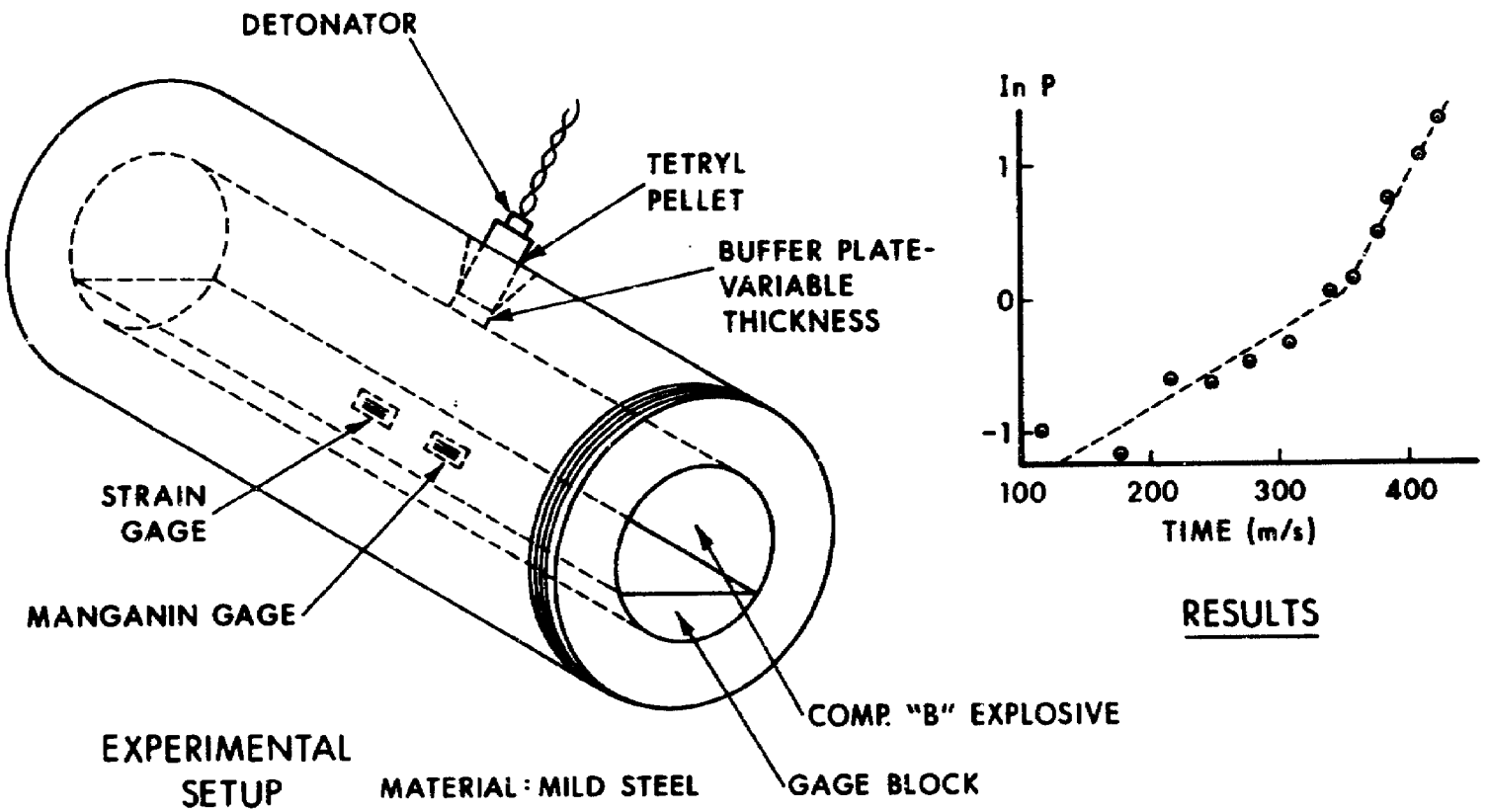

Figure 11. Test Configuration and Typical Result for Frey's Pipe Bomb Experiments

and "no reaction", as evidenced by post test examination, will result if

- ignition did not occur

or

- if adequate deformation did not occur

or

- if sufficient venting occurs as a result of casing fracture or perforation to quench the reaction.

For construction of a model, the following specific assumptions are made.

1. Axial variations in casing thickness and radius can be neglected.

2. The acceptor warhead casing motion can be treated as the motion of a thin shell, the thickness of which corresponds to the warhead casing thickness at its thinnest point*.

3. Strain in the explosive is determined by the casing deformation.

4. Ignition occurs as a result of the stress in the explosive exceeding some critical value.

5. Once ignition occurs, a critical strain in the explosive must be exceeded in order to attain a violent reaction.

The degree to which assumption 1 is met varies considerably from shell to shell. The 105mm HEP warhead meets it fairly well. This warhead has a zone approximately 20 cm long, extending from the rotating band toward the nose, in which both radius and wall thickness are relatively constant. The 105mm HE shell has a zone approximately two-thirds of its length for which it is cylindrical, also. However, its wall thickness varies considerably. The 155mm and 175mm shell have constant radii over less than half their length. The reasons this assumption is made are twofold: It permits application of an analysis of the motion of right circular cylinders made by Huffington, and it permits one to simplify greatly the treatment of explosive product loading upon neighboring shells[17].

*For nearly all shells, this point occurs just above the bourrelet, which is also the point where the most severe loading occurs. Shells which are thin enough to be treatable by thin shell theory still provide enough confinement to the explosive to modify its post ignition response.

[17] *Huffington, N., J of Engineering for Industry, Trans ASME, p 1311, Nov. 1975.*

There are two parts to assumption 2. It is assumed that the thin shell analysis of Santiago[18] can be applied to shells with diameter/wall thicknesses ratios (D/h) of interest here. This is probably not a bad assumption, although most warheads are at the outer limit of applicability of the theory*. The second part of this assumption is that the casing response correlates well with the casing response of a uniform thickness cylinder. Probably this assumption would break down if quantitative deformations were required. Since we require only correlations between different shells, it is deemed adequate.

Assumption 3 is realistic, in view of the fact that the explosive is very weak in comparison to the steel. Thus, elastic deformations in the steel (for example) will produce plastic deformations in the explosives.

Assumption 4 is consistent with assuming that the reaction rate is strongly temperature dependent, i.e., a critical ignition temperature exists. While the measured ignition temperatures for most explosives are not truly constant, they are very slowly varying functions of pressure, etc. and this assumption is reasonably valid.

Assumption 5 has the weakest supporting evidence of any listed here. Qualitatively, available data support this assumption, but little quantitative data exist**,[8,14].

A. The Response of The Casing

Huffington, in his parametric study of the response of structural shells, looked at the effect of geometry, loading, and material properties for the specific case of a fixed end cylinder subjected to a "frontal cosine" distribution of impulsive loading. The geometry is shown in Figure 12. The mathematical formulation is non-linear in the equations of motion, non-linear in the elastoplastic stress-strain relations, and non-linear in the strain displacement relations. The shell was assumed to be thin ($D/h \gg 1$) and of uniform thickness, and Kirchhoff's hypothesis is applicable. (Kirchhoff assumed that the deformation of the shell is such that particles located on a normal to

---

[18] *Santiago, J., BRL Report No. 1571, (1972).* (AD #740742)

**Huffington studied D/h of 50, 100, and 500. He believes the theory is not applicable much below 50. Typical warhead values are 10.3 (105mm HE), 26 (105mm HEP), 7.87 (90mm HE), 10.84 (155mm HE).*

***Extinction of reaction, due to casing failure or perforation, has been a problem during testing, as it can lead to erroneous conclusions as to whether reaction occurred. In some fragment impact tests, where the fragment perforated the case, there was no post-test evidence of reaction. However, high speed photography clearly showed transient burning of the explosive. Such reactions are masked in interround communications tests by the fireball of the donor charge.*

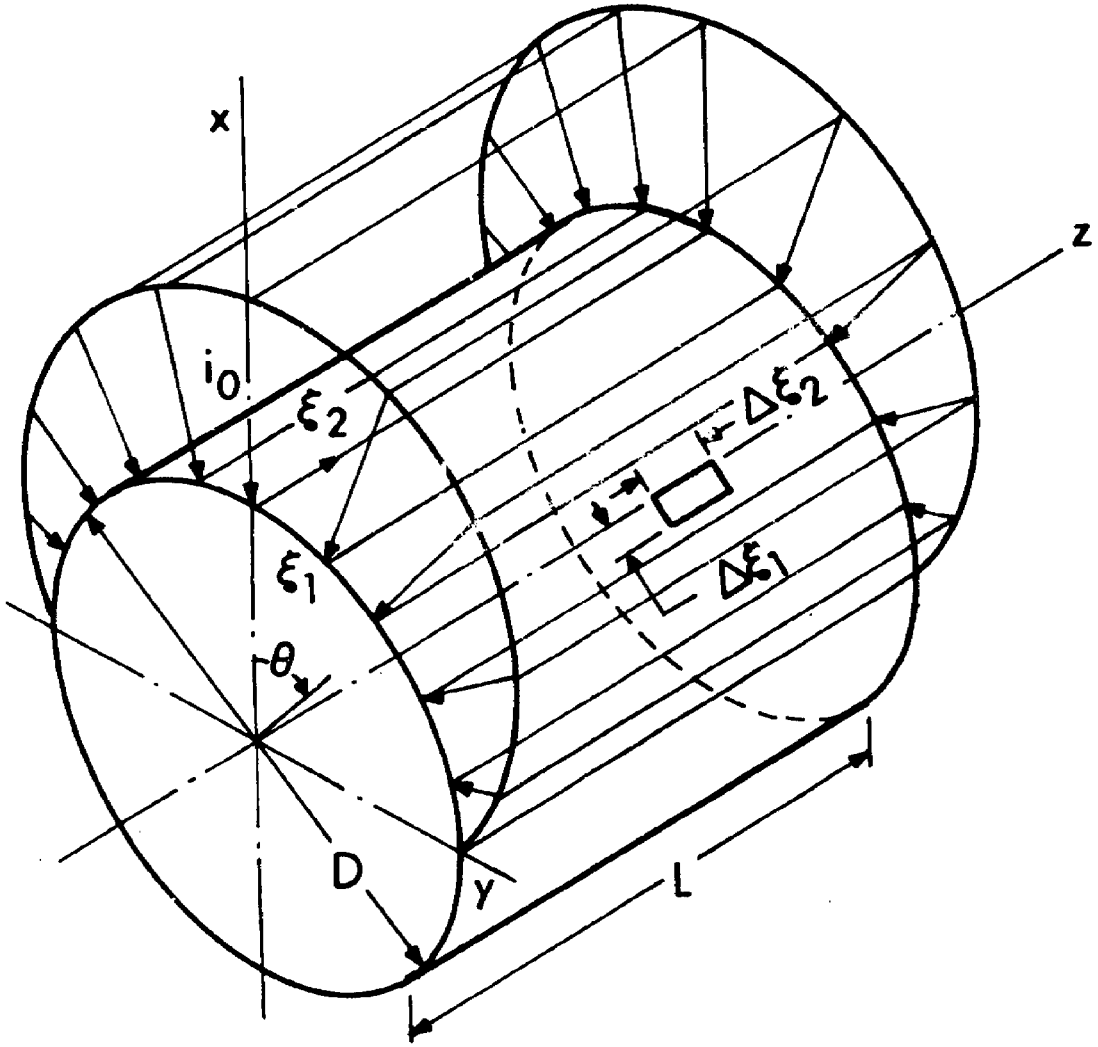

Figure 12. Geometry used by Huffington to Study Response of Thin Shells to Impulsive Loading

a reference surface remain on that normal during deformation, and their distance from the reference surface remains unchanged[18]). An elastic, perfectly plastic model was used, with a von Mises yield criterion. The functional dependence of the radial deformation was expressed as

$$r = f(D, L, h, E, \nu, \sigma_o, C_o, i_o, t)$$

where

r = radial deflection,

D = midsurface diameter,

L = length,

h = casing thickness,

E = Young's modulus,

ν = Poisson's ratio,

σ_o = uniaxial yield stress,

i_o = peak impulse density,

t = time,

C_o = longitudinal wave speed.

These parameters were expressed in terms of seven non-dimensional ratios:

$\pi_1 = r/D$ = non dimensional radial deflection,

$\pi_2 = L/D$ = length to diameter ratio,

$\pi_3 = \frac{i_o C_o}{E h}$ = a scaled impulse density,

$\pi_4 = D/h$ = diameter to thickness ratio,

$\pi_5 = E/\sigma_o$ = ratio of Young's modulus to yield stress,

$\pi_6 = \nu$ = Poisson's ratio,

$\pi_7 = \frac{c_o t}{D}$ = time scaling parameter.

The behavior of the solution was explored by varying one π term at a time, holding others constant. This parametric analysis neglected transient responses; i.e., the seventh π term was omitted. A standard case, with moderately large deflections and elastoplastic response was chosen, with π - values (π_2, π_3, π_4, π_5, π_6) = 1, 0.02916, 500, 238.6, 0.30. These values were chosen because π_2 and π_4 are typical of missile

and reentry vehicles, π_3 corresponds to i_o = 400 Pa.s applied to a thin (1.016mm) aluminum cylinder, and π_5 and π_6 are appropriate for 6061-T6 alloy.

Huffington's results pertinent to this model are shown in Figures 13 and 14. Note that both the maximum response, π_1, and the residual response π_1 are strong functions of the impulse intensity and that these functions are only weakly dependent upon π_2 and π_4. This weak dependence of π_1 upon π_2 (= L/D) and π_4 (= D/h) for a range of π_2 which brackets π_2 or borders π_4 conventional artillery shell, indicates that assumption 3 is well founded at least with respect to shell response; that is $\pi_1 \approx g\ (\pi_3)$.

As stated earlier, we have assumed that ignition occurs as a result of exceeding a critical stress level in the explosive. This stress level is usually exceeded as a result of fragment impacts in the casing. A plot of the pressure generated in Composition B versus the impact velocity of a steel, aluminum, or polyethylene fragment is shown in Figure 15, where attenuation of the pulse due to rarefactions and divergence are neglected. The minimum pressure for ignition of confined Composition B by fragment impact is unknown, but it is estimated to be 2 GPa for munitions interactions.*

The post ignition response of the explosive can be considered as a tradeoff between increasing internal pressure as a result of chemical reaction and depressurization as a result of casing perforation by a fragment, or casing rupture. Any condition which increases the chemical reaction rate of the explosive will favor violent reaction. Thus, heavy confinement, decreased particle size both tend to produce violent reactions. The latter factor is the basis for choosing a deformation criterion for violent reaction. The assumption is that, for a given explosive with a given confinement, violent reaction occurs when a critical energy release rate is exceeded, and the energy release rate is strongly a function of the degree of deformation to which the explosive is subjected.** Figures 13 and 14 show clearly that the radial deformation (π_1) of a thin shell impulsively loaded is proportional to i/h (π_3). Thus, assumption of a critical deformation for violent reaction is tantamount to assuming a critical value of i/h.

---

*Under high rates of deformation, the stress level required for ignition approaches zero - see Susan test data, for example[19].

**The rate of deformation should also be important. For example, Frey has suggested that intergranular motion causes viscous or frictional heating, and the temperature rise is a function of the relative velocities of the grains. Thus, secondary ignition sites can occur within the explosive, as a result of rapid deformation[16].

[19] Dobratz, B., UCRL 51319, Univ. of Calif., (1972).

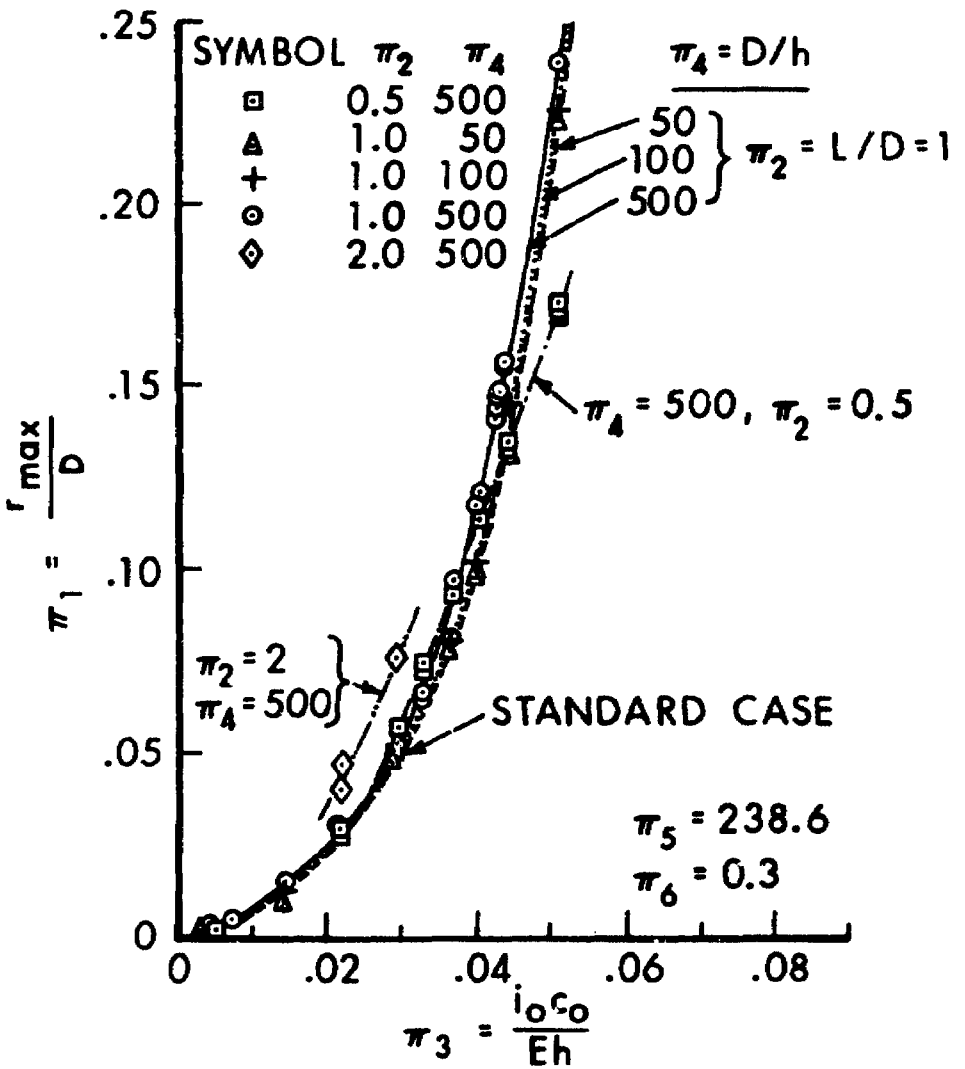

Figure 13. Maximum Radial Deflection of Casing as a Function of Scaled Impulse

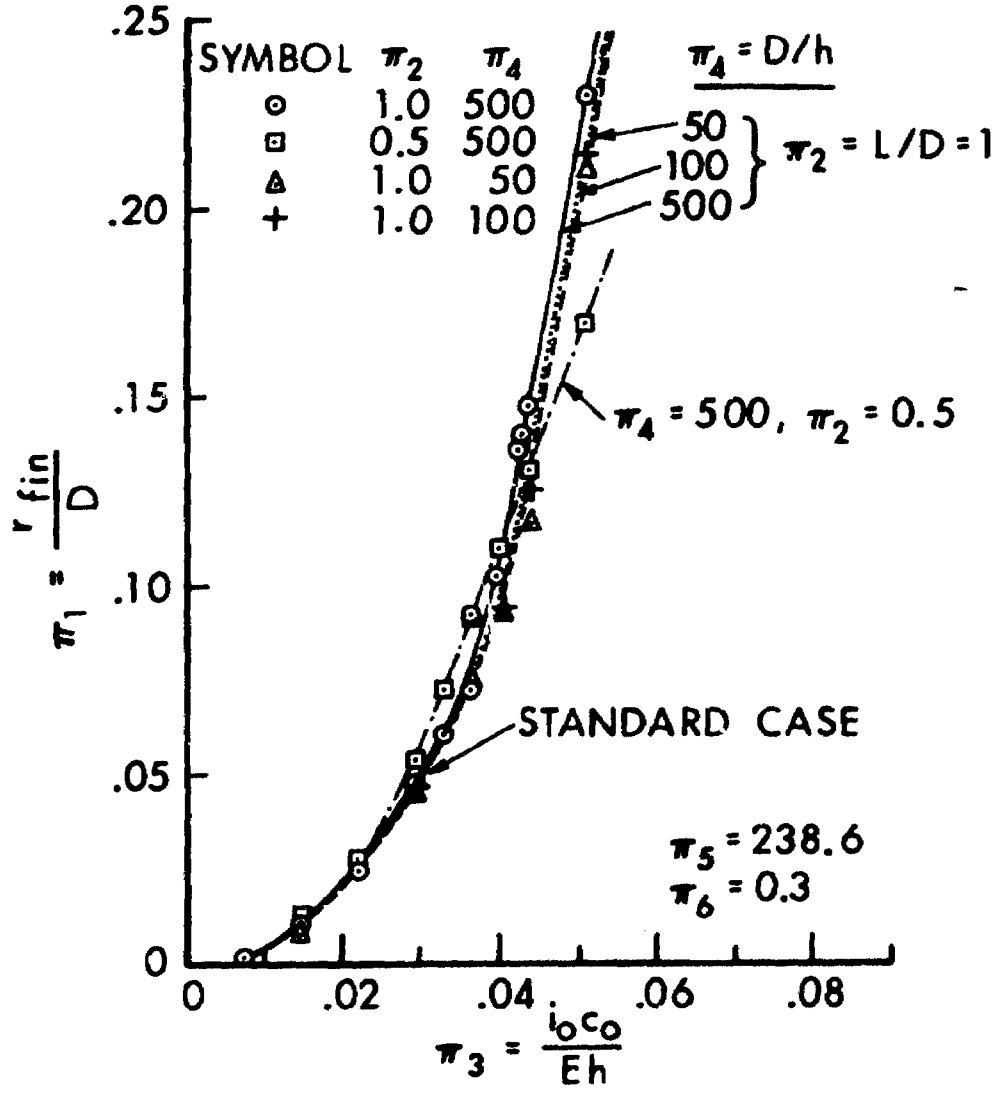

Figure 14. Residual Deflection of Casing as a Function of Scaled Impulse

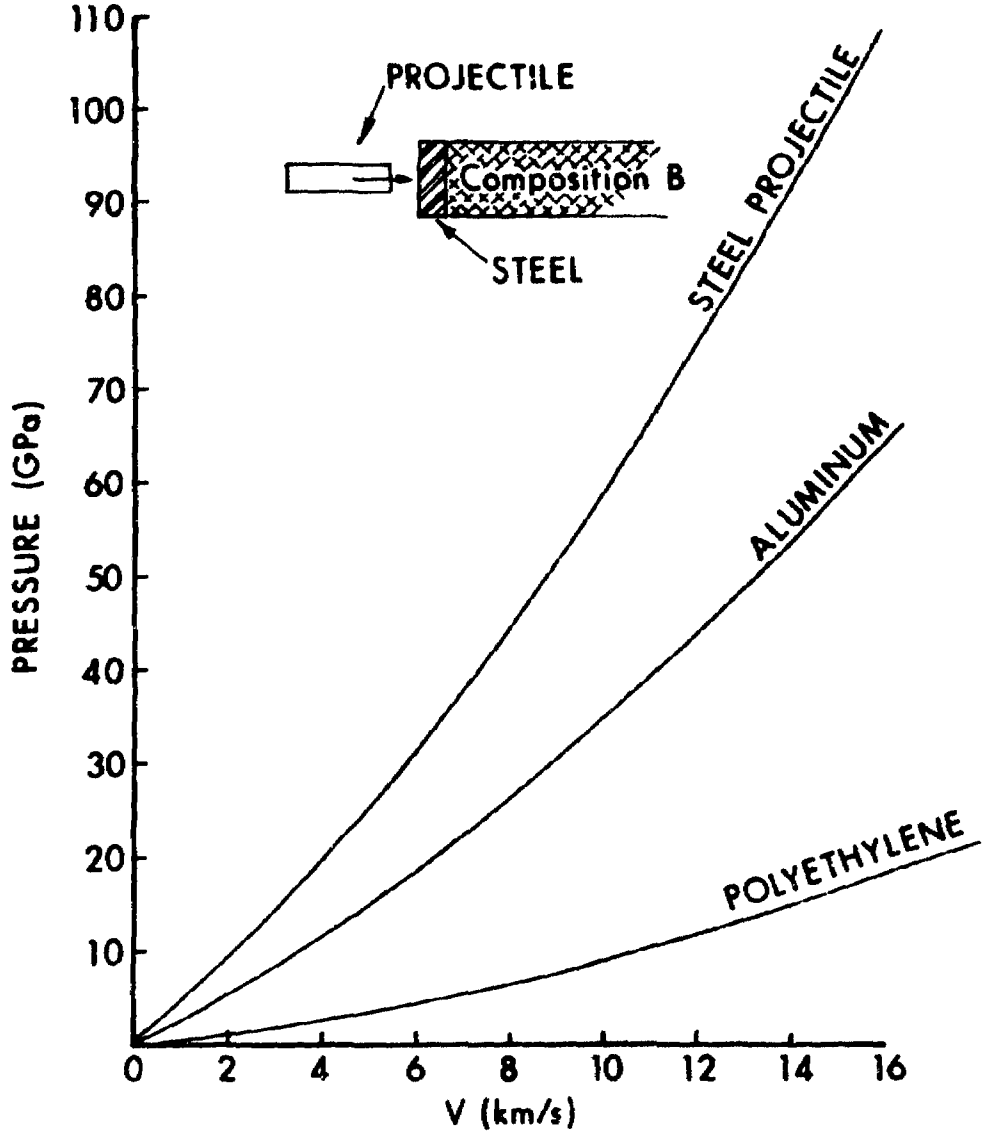

Figure 15. First Shock Pressure Generated at Casing - Explosive Interface versus Impact Velocity for Various Impactors

A series of experiments was sponsored by this author to determine the 50% threshold separation for violent reaction of various warheads subjected to the loading from a deliberately detonated donor warhead. The test setup used is shown in Figure 16. The level of reaction of the acceptor warhead was determined by inspection of the fragments and by examination of the 2.5 cm thick steel witness plate. The criterion for a violent reaction was that the acceptor perforate the witness plate. Thus, for this instance, no significant distinction is made between violent reaction and detonation. Test results and calculated data are presented in Table III. Fragment kinetic energy/area, E, and momentum/area, P, were calculated using the Gurney velocity formula for cylindrical charges[20] given by the equation

$$V = (2E^*)^{1/2} \left[\frac{M}{C} + \frac{1}{2}\right]^{-1/2}$$

where

V is the fragment velocity,

$\sqrt{2E^*}$ is the Gurney constant (values are presented in Table III),

M is the mass of steel casing,

and C is the mass of explosive.

Thus, the areal fragment kinetic energy delivered to the acceptor is given by

$$E = \frac{2E^* M}{2\pi R\left[\frac{M}{C} + \frac{1}{2}\right]} = \frac{E^* M}{\pi R\left[\frac{M}{C} + \frac{1}{2}\right]}$$

where R is defined by Figure 16, and

$$P = \frac{M\sqrt{2E^*}}{2\pi R\left[\frac{M}{C} + \frac{1}{2}\right]^{1/2}},$$

where P is the fragment momentum per unit area. The values of i_o are proportional to the impulse delivered to the acceptor by the donor explosive, and were calculated in the following way:

---

[20] *Henry, I., "The Gurney Formula and Related Approximations," a presentation to the American Ordnance Ass'n, April (1967), DDC AD 813398.*

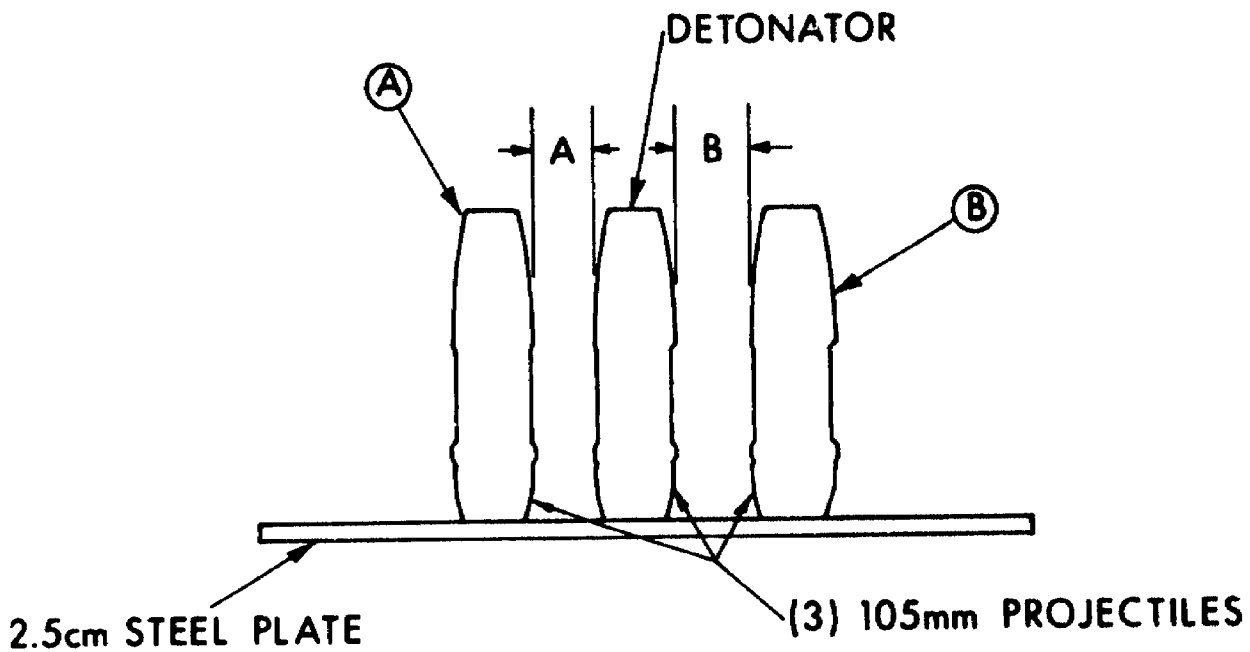

Figure 16. Schematic of Test Setup used to Determine 50% Separation Threshold for Violent Reaction of 105mm Shell

Table III. Values of Gurney Constants for Various Explosives*

Explosive	$\sqrt{2E^*}$ (M/S)
Baratol 33%$_w$ TNT, 67% $BA(NO_3)_2$	1585
Tritonal 20%$_w$ Al, 80% TNT	2195
TNT	2438
HBX-1 11%$_w$ TNT, 67% Comp B, 17% Al, 5% D-2 Wax	2469
Comp B 40%$_w$ TNT, 60% RDX	2682
Cyclotol 30%$_w$ TNT, 70% RDX	2701
25%$_w$ TNT, 75% RDX	2713
Comp A-3 9%$_w$ wax, 91% RDX	2743
RDX 3%$_w$ wax, 97% RDX	2835
100% RDX	2835
Black powder 10%$_w$ S, 16% C, 74% KNO_3	945

*Data from Reference 20.

The specific kinetic energy of the explosive products, E_{HE}, is given by

$$E_{HE} = \frac{\bar{V}_{HE}^2}{2}$$

where $\bar{V}_{HE}$ is the average product velocity. E_{HE} is proportional to the Gurney E*, so

$$\bar{V} \propto \sqrt{2E^*}$$

and the areal impulse to acceptor casing thickness ratio

$$\frac{i}{h} \propto \rho \frac{R_o^2 \sqrt{2E^*}}{R_h}$$

where R_o is the radius of the explosive charge, and h is the wall thickness of the acceptor. Thus the critical deformation condition implies that

$$\frac{R_o^2 \sqrt{2E^*}}{h} \text{ vs R be linear.}^*$$

The data are plotted in Figure 17.

A regression analysis of R onto each of the parameters in Table IV was made, and the correlation coefficients are shown in Table V. Note that R correlates extremely well with i/h, but does not correlate significantly with any of the fragment parameters.

---

*For predicting the 50% threshold separation for RDX bared explosives, the scaling law follows:

$$R_2 = R_1 \left(\frac{R_{o2}}{R_{o1}}\right)^2 \left(\frac{\sqrt{2E_2^*}}{\sqrt{2E_1^*}}\right)\left(\frac{h_1}{h_2}\right)$$

where R_1 is the known threshold separation for a warhead pair, the donor of which has a charge radius R_{o1} and a Gurney constant $\sqrt{2E_1^*}$, and the acceptor of which has a wall thickness h_1. R_2, R_{o2}, h_2, and $\sqrt{2E_2^*}$ are the corresponding parameters for the unknown.

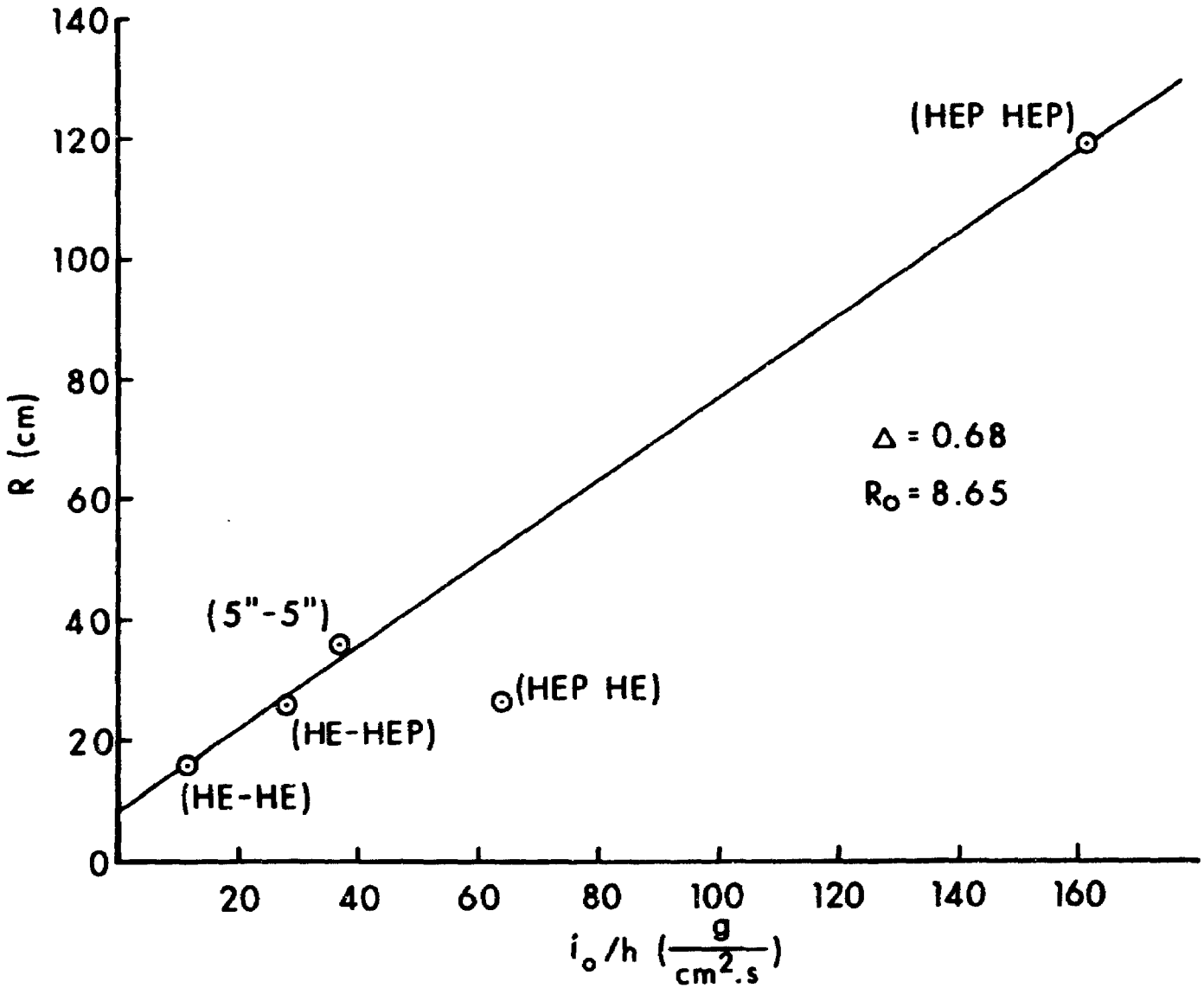

Figure 17. A Plot of the 50% Threshold Separation versus a Scaled Areal Impulse Density

Table IV. Calculated and Measured Parameters Associated with Interround Communication Experiments

Donor	Acceptor	R R(cm)	E_f Fragment KE/Area $\left(\frac{gm}{cm^2}(m/s)^2\right)$	P Fragment Momentum/Area $\left(\frac{gm}{cm^2}\ m/s\right)$	i Explosive Impulse/Area $\left(\frac{gm}{cm^2}\ m/s\right)$	h Acceptor Casing thickness (cm)
105 M1 HE	105 M1 HE	17.8	5.6×10^8	3.6×10^5	11.3×10^3	1.02
105 M1 HE	105 M393A1E1 HEP	25 ± 5	5.6×10^8	3.6×10^5	11.3×10^3	0.4
105 M393A1E1	105 M1 HE	26	5.7×10^8	2.4×10^5	64.5×10^3	1.02
5" 54	5" 54	35.4	3.7×10^8	4.1×10^5	60.6×10^3	1.65
105 M393A1E1	105 M393A1E1	119.3	5.7×10^8	2.4×10^5	64.5×10^3	0.4

Table V. Correlation Coefficients for Regression of R on Various Parameters

	R	E	P	L	E/h	P/h	i/h
R	1.000	0.158	-0.548	0.524	0.557	0.227	0.960

A priori, one would expect that the major contribution to the initiation of the acceptor would be made by the fragments from the donor. Fragments are much more efficient than airshock or explosive products at delivering energy to the target, and peak pressures generated in the target are much higher from fragment impact than from explosive products, due to the fragment's much higher shock impedance. Thus, it was quite startling that there was negligible correlation between fragment parameters and acceptor response. The interpretation that this author espouses is that the fragments control ignition*, but in the range of warhead separations investigated, the probability of the acceptor warhead being impacted by an ignition causing fragment is essentially unity. The fragments have little influence in the post ignition response because, although they cause cratering and sometimes perforation, the areal density is usually insufficient to cause massive deformation of the target. Thus, although the fragments cause severe local deformation to the casing, the damage to the explosive is generally not severe enough to enhance reaction greatly.

The situation discussed above would change with increasing fragment mass and velocity; eventually an individual fragment would be energetic enough to cause massive deformation over a significant volume of the target, with consequent violent reaction. Such is the case for threshold data from gun firings where there is no loading from explosive products and where the response of the target is to impact by single fragments.

Reeves' data (Reference 11) covered fragment masses from 1.94 gm to 15.55 gm, impacting against Composition B loaded 105mm M1 HE warheads. We sponsored acquisition of additional data for identical targets, with fragments ranging from 75 gm to 300 gm. All fragments were steel, right circular cylinders, with L/D = 1. The response of the targets was inferred from post firing examination of a 1.5 cm steel witness plate, and from recovery of the target fragments. The criterion for a violent reaction was perforation of the witness plate. All data were obtained

That the fragments play an important role in the initiation process was demonstrated by the following: The 50% separation distance for a 105mm HEP acceptor and a bare charge donor, of total weight and geometry similar to a HEP warhead, was measured. The separation threshold for the bare charge donor was 3.1 cm, as opposed to 119.5 cm for the HEP donor.

via the up and down method for small samples[21]. (The data, with Reeves' data, are plotted in Figure 9). The fact that both sets of data fall in a single smooth curve is reassuring, and indicates that no experimental artifacts have been introduced as a result of different lots of explosive and different experimenters. It is reasonable to expect that the fragment impact initiation of violent reaction (not classical shock initiation!) will obey the same mechanism as does interround communication. If so, the criterion for initiation of violent reaction is that a critical areal impulse/casing thickness ratio be exceeded. Thus, we have for the 50% threshold locus of mass versus impact velocity

$$\frac{mV}{Ah} = \text{constant}.$$

However,

$$\frac{mV}{Ah} = \frac{\rho \ell V}{h}$$

$$\frac{\ell}{D} = 1 \Rightarrow \ell = 2r$$

$$\frac{mV}{Ah} = \frac{2\rho r V}{h}$$

but

$$r = \left(\frac{m}{2\rho\pi}\right)^{1/3}$$

so that the criterion becomes

$$\frac{2\rho V}{h}\left(\frac{m}{2\rho\pi}\right)^{1/3} = \text{constant}$$

or

$$\frac{m^{1/3} V}{h} = \text{constant}.$$

---

[21] *Dixon, and Massey, Introduction to Statistics, 3rd Edition (1971).*

The data of Figure 9 are replotted in Figure 18, where the h is suppressed. The solid curve is a straight line with a slope of -3, and it can be seen that the fit is good for over three decades change in mass. This provides very strong support for a mechanism which leads to an areal impulse criterion for initiation of violent reaction. Note that an energy criterion is inconsistent with these data.

V. SHIELDING TECHNIQUES

Concurrently with the mechanistic studies discussed in the previous section, experiments and analyses were conducted to reduce the probability of propagation of detonation. Initially, attention was given to prevention of mass detonation. As we shall soon see, for several important applications, prevention of mass detonation is not sufficient. One must also prevent sequential detonation and violent reactions.

Anderson and Rindner, in 1973, published a report on shielding of 155mm projectiles[22]. They found that 2.5 cm steel or 5 cm thick aluminum plates and bars emplaced between rounds were effective in preventing propagation of detonation at interround separations down to S = 23 cm.* We took a similar approach, rather than investigate sleeves, for example, because it was clear that the latter were less weight efficient. Using steel tube, or PVC rod (PVC has a much lower shock impedance than steel, and thus delivers a much weaker shock to the acceptor for the same impact velocity), we have been able to prevent mass detonation of Composition B loaded 105mm M1 HE and Composition A-3 loaded M393A1E1 HEP warheads, where the interround separation, S, was as small as 5 cm. In nearly all cases, considerable damage occurs to the acceptor. In the case of the HEP warhead, which has a very thin skin, it is very difficult to prevent the acceptor from breaking open. This, of course, creates a considerable problem with fires. A typical test configuration is shown in Figure 19. All shields were free standing. A variety of different shield materials and geometries were tested, for both the M1 HE and the M393A1E1 HEP warheads. Configurations and results are presented in Table VI. The data indicate that the principal shielding mechanism involved was shadowing the acceptor from primary fragment impacts from the donor warhead. Figure 20 shows graphically the role of the shield as shadower. The various frames show fragments from 10.5 cm diameter, Composition B loaded steel cylinders interacting with shields (mild steel tube, 4.2 cm OD, 3.2 cm ID) and 10.5 cm diameter acceptors. The shields very effectively prevent primary fragment impacts upon the acceptors. In this particular shielding configuration, violent reaction of the acceptor would occur, because of insufficient shield integrity. A slightly heavier gauge shield (4.2 cm OD, 2.3 cm ID) was successful in preventing violent reaction of the HEP acceptors.

---

[22] *Anderson, C., and Rindner, R., PATR 4425, (1972).*

**See Figure 16 for definition of S.*

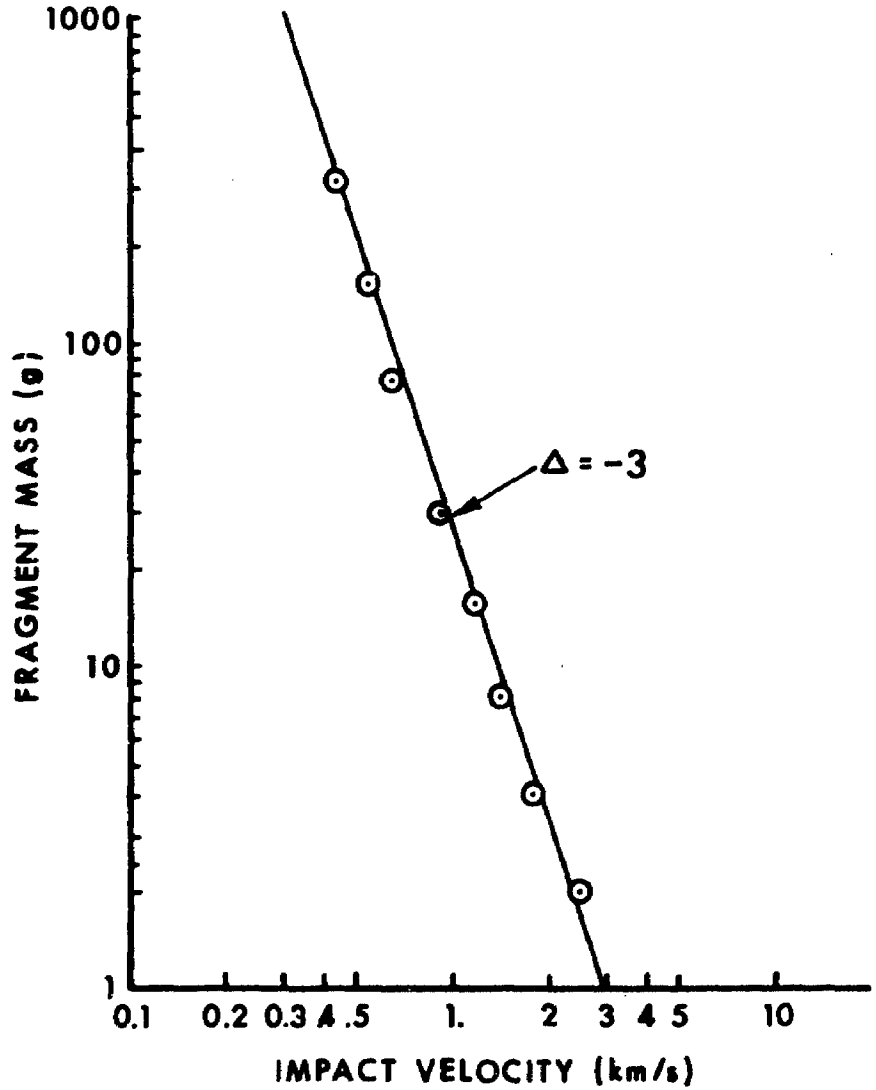

Figure 18. Fragment Impact Initiation of 105mm HE Shell, Replotted to show that Areal Impulse Criterion Applies

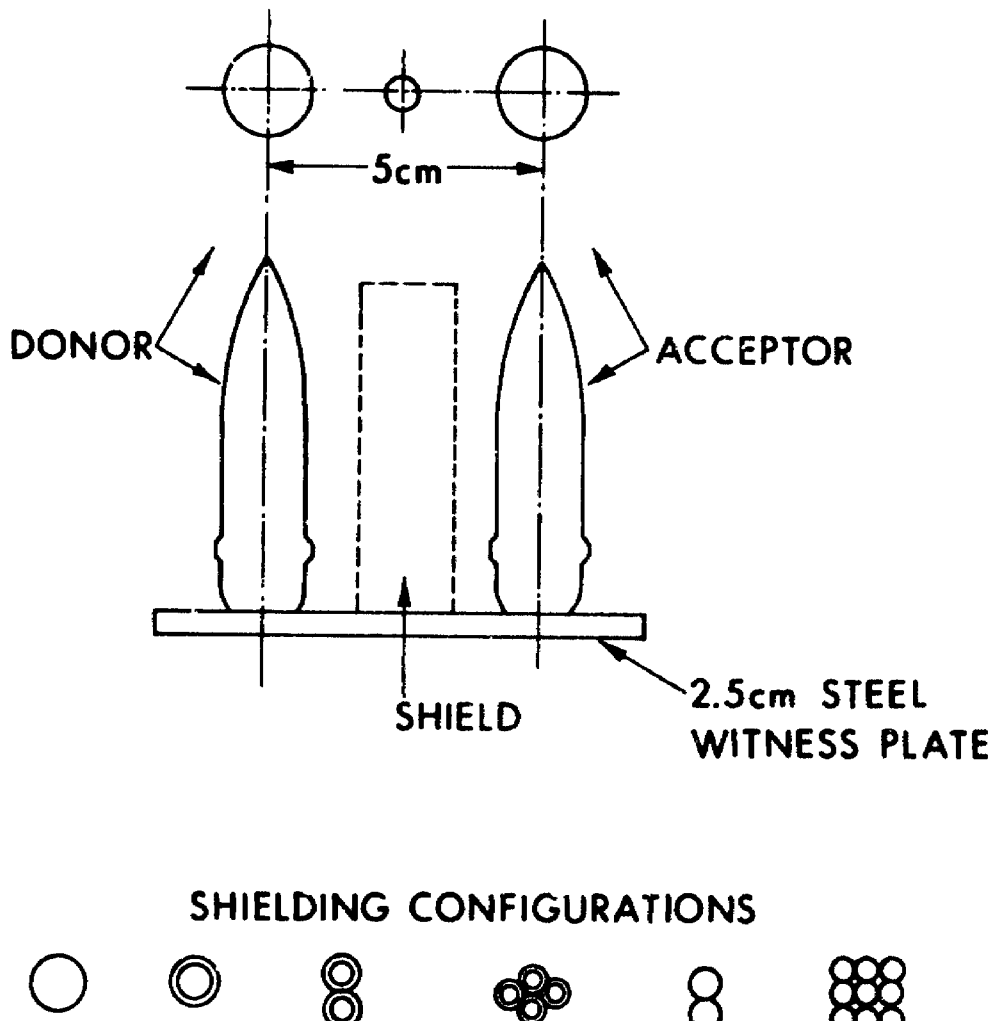

Figure 19. Schematic of Test Configurations for Evaluating Shield Efficiencies

Table VI. Shielding Data for 105mm M1 and M393 Rounds

Shielding Material	Mass (Kg)	Projected Dia. (mm)	Prevented Burn of HE in Acceptor	Prevented Detonation of Acceptor
		105 M1 HE		
1 ea. solid Al rod	6.01	38.1	yes	yes
1 ea. steel pipe	1.27	33.3	no	yes
1 ea. steel pipe	1.72	42.2	no	yes
1 ea. steel pipe	2.05	48.3	no	no
1 ea. steel pipe	1.63	33.4	yes	yes
1 ea. steel pipe	2.76	33.4	yes	yes
1 ea. steel pipe	1.11	26.7	no	yes
1 ea. steel pipe	1.30	21.3	no	yes
1 ea. steel rod	3.46	33.3	yes	yes
1 ea. hardwood dowel	0.45	38.1	no	yes
2 ea. steel pipe	2.54	66.6	no	yes
4 ea. steel pipe	1.28	27.4	no	yes
4 ea. steel pipe	0.74	20.3	no	yes
2 ea. steel rod	1.90	34.9	yes	yes
1 ea. steel rod	0.95	17.4	no	yes
12 ea. steel pipe	2.21	41.2	no	yes
		105 M393A1E1 HEP		
1 ea. steel tube	2.26	42.2	no	no
1 ea. steel tube	3.93	42.2	yes	yes
2 ea. steel rod	1.90	35.0	no	yes
1 ea. steel tube	2.75	48.3	no	no
1 ea. wood dowel	0.31	38.1	no	no
1 ea. PVC rod	0.65	38.1	yes	yes
1 ea. steel rod	3.13	38.1	no	no

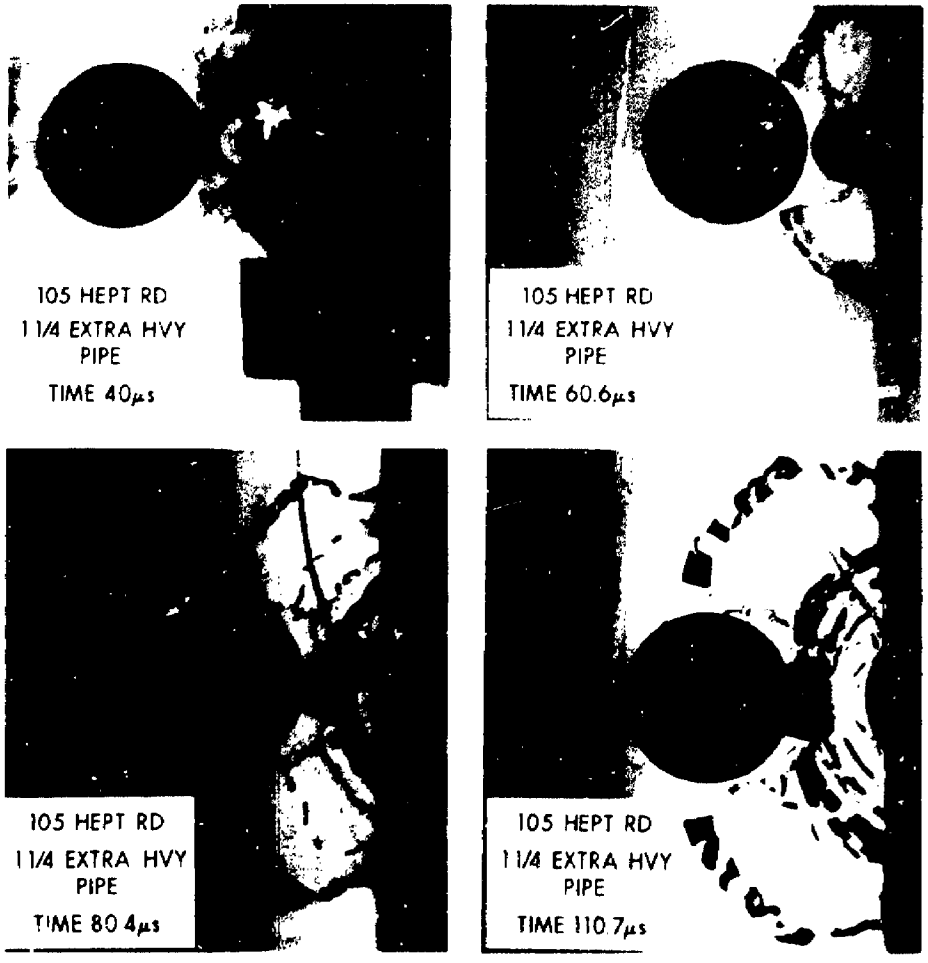

Figure 20. Sequence of Radiographs (Four Different Experiments!) Showing Effectiveness of a Shield as Fragment Shadower

It can be inferred from Table VI that it is relatively easy to protect the M1 HE shell such that there is no reaction; but it is difficult to prevent reaction of the M393A1E1 HEP warhead. Indeed, nearly all shields tested with the M1 warheads were successful, and shield geometry and material did not play a significant role, over the range tested. While some shield configurations were very effective in preventing detonation or violent reaction of the HEP warheads, in nearly every instance the acceptor warheads were massively deformed and the casings split open. In nearly every instance some explosive was lost, either through reaction or through breakup and spillage.

The results above are consistent with the mechanisms described in the previous section. For both warhead types the shields are effective in preventing primary fragment impact and, hence, ignition of the acceptor. However, the shields are ineffectual in preventing massive deformation and splitting open of the thin skinned HEP rounds. Since both ignition and deformation are required for detonation or violent reaction, the shields were effective in preventing immediate violent reaction or detonation of the acceptors. The damaged HEP warheads are clearly vulnerable to any ignition source which is presented at a later time, however. Thus, in order to prevent sequential detonation or violent reactions after the first event, it is necessary to prevent splitting of the warhead casing.*

All the tests described above were one-on-one donor and acceptor, and no provisions were made for nearest neighbor interactions. Several tests with M1 and with M393A1E1 warheads were made using the configuration shown in Figure 21. These configurations permitted observing (a) the possibility of primary fragments ricocheting from vicinal warheads to hit an acceptor and (b) acceptors being hit by shields and then being forcibly thrown into another shield and warhead. The change in configurations introduced no change in results. Experiments using wax filled acceptors gave no indication of damage to acceptors from fragments. The deformation of inert loaded warheads separated by the acceptor from the donor suffered less damage than the acceptor, as might be expected.

With these apparent successes, some scaled up experiments were performed using HEP warheads arrayed as in Figure 22 (the number of warheads involved in each test was determined by the availability of shielding). In all tests, the cross hatched warhead was detonated in

The split warheads are particularly vulnerable to thermal ignition sources, which present the greatest threat. Test photographs show that the fireball lasts for many milliseconds, certainly long enough to ignite exposed explosive in contact with the fireball. Hot metal is in the area long after the fireball has disappeared, of course. It should also be noted that a damaged round with casing intact is still more sensitive to stray fragment impacts than is an undamaged round. No quantitative data exist, however, to illustrate this last point.

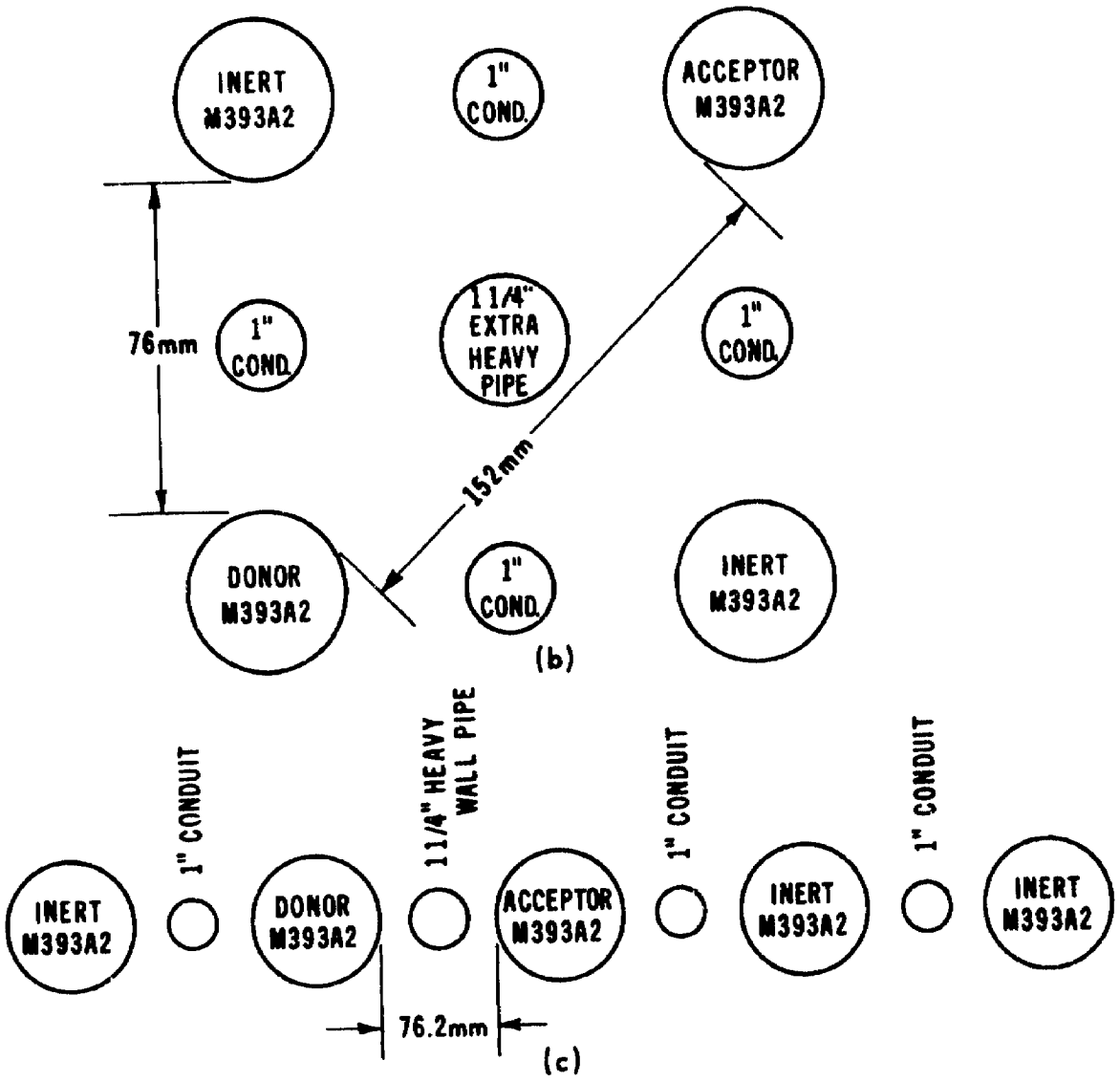

Figure 21. Schematic of Test Configurations used to Determine Nearest Neighbor Effects

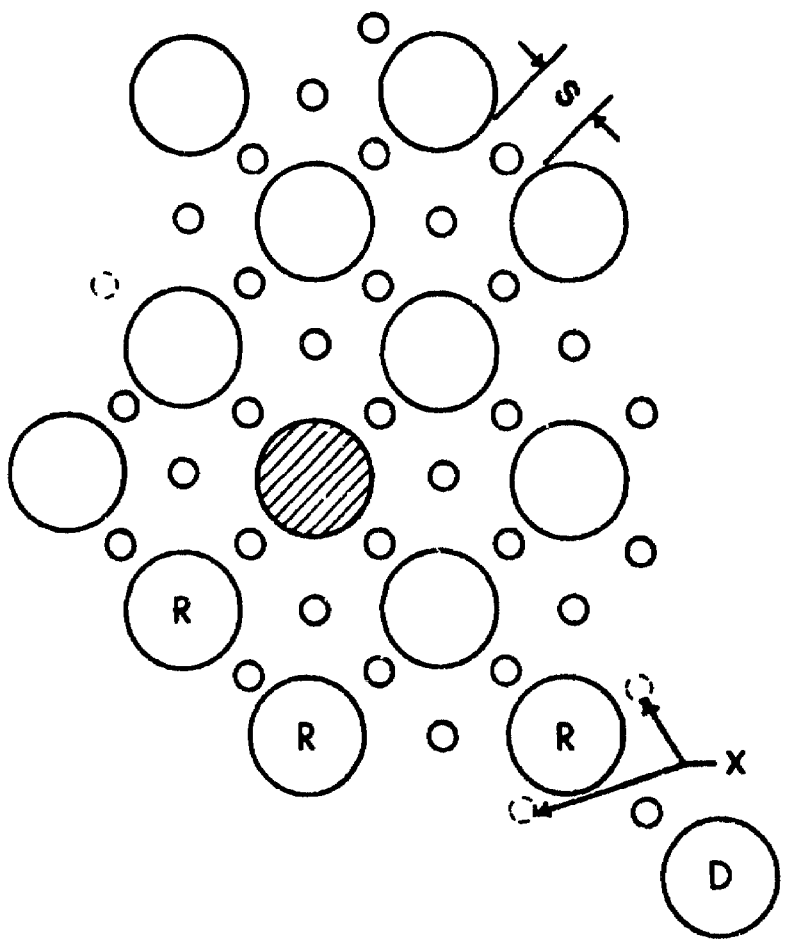

Figure 22. Schematic of Test Configuration for 105mm HEP Warheads

the design mode. The interround separation distance (S) was 5 cm. Shields were 3.8 cm diameter PVC rod. The rounds labeled with "R" reacted sufficiently violently to make a small dent in the witness plate. The warhead marked "D" reacted sufficiently violently to perforate the witness plate. For all practical purposes, the warhead detonated. In the first test, an oversight was made in that shields were not placed at the positions marked with an "x" in Figure 22. This oversight was corrected in the second test, and, also, the interround spacing was increased to 7.5 cm. In the second test, four of the acceptors detonated.

The trend indicated above was not particularily satisfying. An analysis of buffer motion was made and it was found that, depending upon the assumptions made, the terminal velocity of the 3.8 cm diameter PVC buffers was 0.5 - 1.2 Km/s. Measurements were made of the pressure delivered to an explosive simulant by an impacting PVC rod configured as in Figure 23, using manganin gauges imbedded in the acceptor warhead[23]. The pressure (~ 16 Kbar in the explosive) corresponded to ~ 1.5 Km/s impact velocity. The precise value of the shield velocity is unimportant. Its order of magnitude may be extremely important. An unclamped or unimpeded shield traveling at an average velocity of 0.5 Km/s will have moved 0.5 meters in 1 millisecond. This would place any unimpeded shield outside of the test array within one millisecond. For events occuring later than ~ 1 msec after the initial detonation, the shields will be ineffectual in protecting other warheads. Film coverage of the first test was examined very carefully. It was found that there were four sequential explosions, with the last one occurring milliseconds after the donor detonation. While unfixed PVC shields are very effective in preventing mass detonation, they are ineffectual in preventing sequential violent reactions or detonations.

A third test was performed using nearly the same configuration as the previous two, with a HEP interround separation of 7.5 cm. This time, however, 5 cm dia PVC shields were clamped top and bottom. Clamping was obtained by drilling holes in the witness plate (bottom) and a 1 cm steel cover plate (top), through which the PVC rods were inserted. Upon detonation of the donor warhead, all 13 acceptors detonated. In tracing down the source of this egregious failure, it was determined that the warheads used in this test were T81 models which were manufactured in 1952 and stored in Japan. These warheads have been classified unsafe for firing since ~ 1970. They also have a different wall thickness than the M393A1E1, and in excess of a pound more explosive. They thus represent a much more severe shielding problem than the M393A1E1, and little relevant information can be obtained from the third test.

---

[23] *McLouf, C., and Frey, R., private communication.*

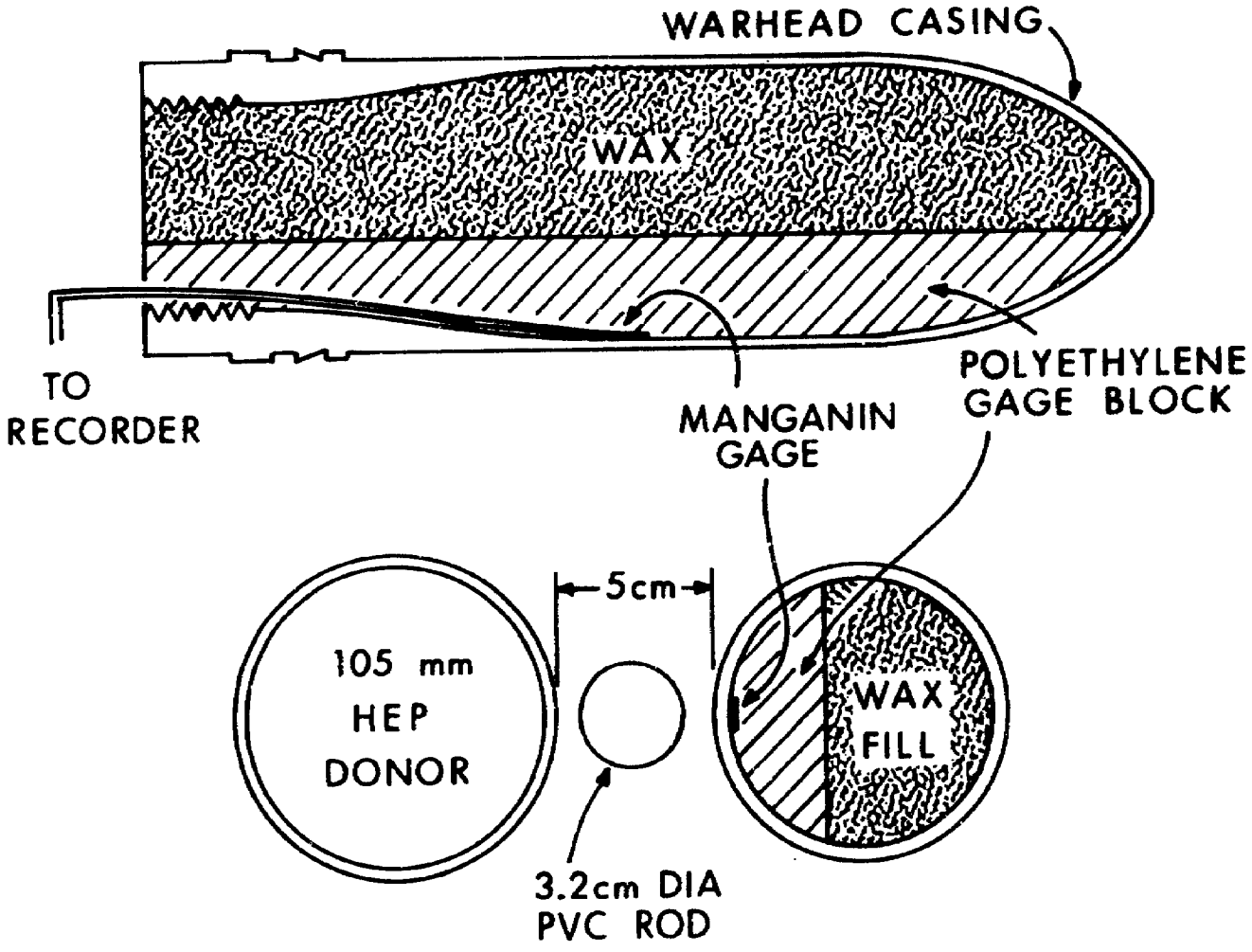

Figure 23. Schematic for Determination of Pressure Delivered to Acceptor Explosive by PVC Shield

The results presented above show that the shields are effective in preventing mass detonation of 105mm M1 and M393A1E1 warheads. The shields are inadequate to prevent massive deformation and splitting of the HEP warheads and are ineffectual in preventing sequential violent reactions or detonations. Presumably, both shield motion (which makes the acceptor warheads vulnerable to subsequent fragment impacts, should a second round go off) and breakup of the acceptors (which greatly lowers the conditions necessary for ignition) are strong contributory factors in sequential reactions.

The assumption was made that splitting of the warhead casing results from a buildup of internal pressure during the deformation process. Thus, an attempt was made to use sleeves which would provide additional stiffness to the warhead. Huffington's analysis indicates that by increasing the effective wall thickness of the warhead casing deformation resistance would be increased. For example, a steel sleeve of wall thickness ~ 1.3 cm (based on 105mm M2 HE results) should be adequate. Monolithic-walled sleeves are not particularly weight efficient and the ring stiffened cylinder shown in Figure 24 was made. This was anticipated to be a gross overdesign. Other, simpler, designs were made to establish a data base. The results, which considerably surprised this author, are presented in Table VII. The effectiveness of the various sleeves in preventing cracking of inert acceptor casings is greater with decreasing outer sleeve thickness and decreasing stiffness. Note, also, that the lightest weight sleeve tested is the most effective. The data base and the author's understanding are inadequate to state conclusively the reasons for these trends. However, the trends are consistent with cracking of the warhead casing by brittle fracture as a result of shock loading, rather than by bursting as a result of internal pressure increase.

The supporting evidence for this mechanism of failure* is strong. A 105mm M1 HE shell (wax filled) which had failed when subjected to the environment created by another HE shell detonated at S = 12 cm was subjected to fractographic analysis by Dr. G. Moss. The details of his analysis are attached as Appendix A of this report. The most important conclusions are that (1) incipient spall occurred on the impacted casing; (2) the casing failed, beginning at the spalled region; (3) in the absence of the spall, the casing probably would not have failed; (4) the spallation could be prevented by reducing the input stress level. Thus, for this type of warhead, casing failure could be prevented by using low shock impedance shields.

Suggested by Dr. G. Moss, of this laboratory.

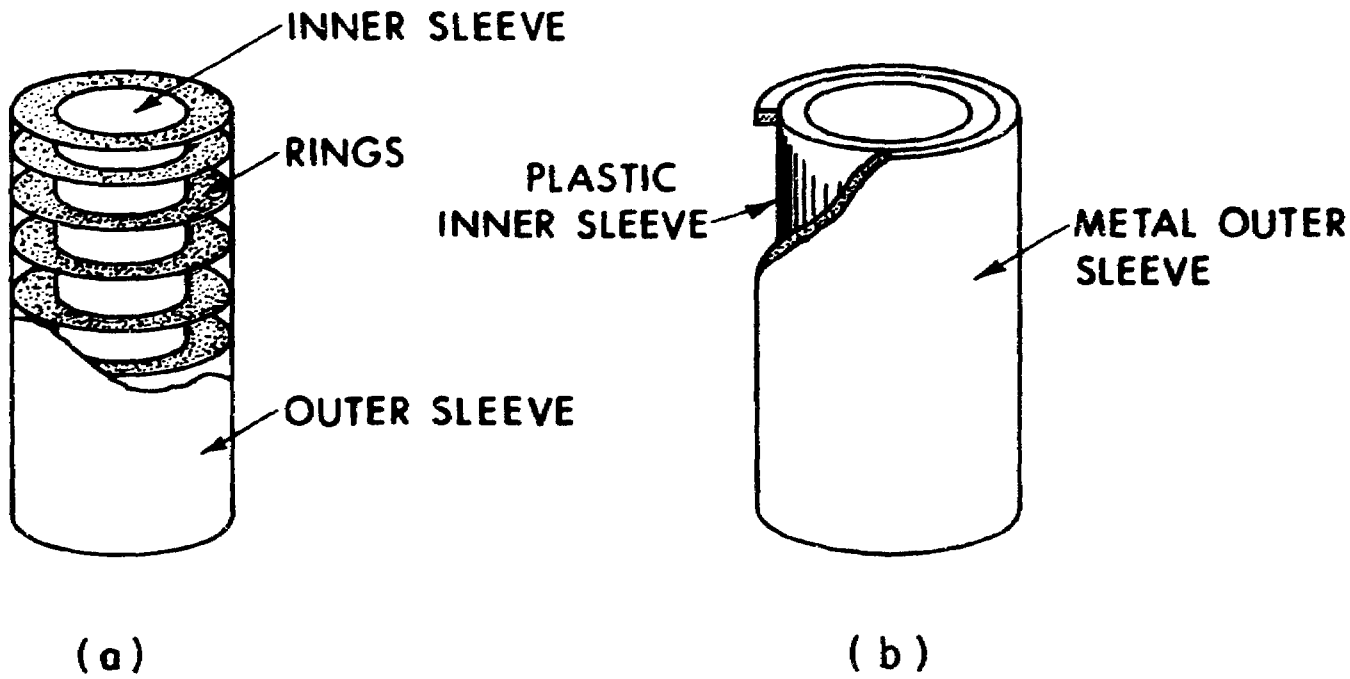

Figure 24. Configurations Tested to Prevent HEP Warhead Breakup

Table VII. Sleeve Data for 105mm M393 Rounds

Configuration	Outer Sleeve OD(cm)	Outer Sleeve wt(cm)	Polyethylene Inner Sleeve wt(cm)	Weight (Kg)	Results
ring stiffened steel cylinder	14.6	1.9	-	10.1	broken end, HE exuded
Concentric Sleeves	15.2	0.6	0.97	14.3	broken, HE exuded
Concentric Sleeves	15.2	1.3	0.97	9.3	broken, HE exuded
Concentric Sleeves	14.0	0.6	0.97	5.5	crack
Concentric Sleeves	13.5	0.4	1.3	4.2	survived intact

VI. SUMMARY AND CONCLUSIONS

The Tooele T-205 milvan storage test results were analyzed and it was concluded that buffering at the milvan level, to prevent propagation of detonation from milvan to milvan of class 7 stores was ineffectual. This conclusion obtains independent of whether the buffer milvans are inert loaded or filled with non mass detonable stores, and necessitated examination of the means by which detonation and violent reaction are propagated between individual munitions.

Experiments were conducted to determine the mechanisms of interround propagation. It was found that the 50% threshold separation distance, R_{50}, for a donor warhead to cause a neighboring warhead to detonate or react violently correlates strongly with the areal impulse density delivered to the target munition by the explosive products of the donor. The data are consistent with assuming that ignition is caused by individual fragment impacts and the violence of the post-ignition reaction is controlled by the magnitude of the bulk explosive deformation. Since the yield strength of the explosive is so much less than that of the warhead casing, the warhead casing controls the explosive deformation. This leads to a criterion for initiation of violent reaction, the ratio of delivered impulse per unit area to acceptor warhead casing, which is useful in predicting threshold separation distances.

While experiments indicated that fragments greatly influence ignition, no significant correlation between R_{50} and fragment parameters such as areal fragment kinetic energy density or impulse density was

observed. This is explained by assuming that the fragment density delivered to the target was sufficiently great to saturate target response, i.e., ignition was guaranteed under the conditions investigated. In the regime of masses and velocities where individual fragments themselves cause violent reaction or detonation, it was shown that, for right circular steel cylindrical fragments of unity fineness ratio, the data are consistent with the above mentioned initiation criterion for over three decades change in mass.

Experiments with various shield materials demonstrated that it is possible to prevent mass detonation of 105mm M1 HE shell and 105mm M393A1E1 HEP shell, where the shell were placed only 15.5 cm apart, center to center. Shields serve primarily as shadowers, to prevent direct impact of the acceptor by fragments from the donor. Secondly, the shields serve to reduce the pressure transmitted to the acceptor. Thus, low shock impedance materials such as polyvinyl chloride were found to be effective shields. None of the shields were found to be effective, in the configurations used, in preventing sequential violent reaction or detonation of HEP warheads. The shields investigated were unable to prevent massive deformation and breakup of the thin skinned HEP warheads, which were thus vulnerable to any subsequent ignition source.

ACKNOWLEDGMENTS

The author wishes to thank J. P. McLain and D. Collis, of NMIT, Socorro, NM, for gathering much of the experimental data. He is indebted to E. O'Leary of BRL for enthusiastic support in obtaining materials and performing certain tests. The fractographic analysis by G. Moss of BRL was much appreciated and contributed considerably to the author's understanding of warhead breakup. The many discussions and considerable insight provided by R. Frey of this laboratory are especially appreciated. The enthusiastic support of Messrs D. Menne and R. Prenatt was also greatly appreciated.

APPENDIX

SHELL FRACTURE

A. Shell Material

Photomicrographs of unimpacted shell material are shown in Figures A-1 through A-3, and the Rockwell C hardness of this material was determined to be 21. It is apparent from this information that the microstructure is a mixture of pearlite and ferrite (approximately pure iron), and that the material had been previously deformed, presumably in a forming operation.

B. Observations and Conclusions About Projectile Fracture

The surfaces at B (Figs. 4-A and 5-A) are smooth and shiny, indicative of extensive shear. This is different from the dimpled surfaces characteristic of spallation from flat parallel plate impacts.

There do not appear to be enough independent surfaces at B to correspond with the void nucleation rates that should apply to the ferrite during spallation. Experimental results for Armco iron, which is approximately the same as the ferrite of the projectile, indicate the nucleation rate $\dot{N}$ can be approximated with the expression

$$\dot{N} = \dot{N}_o \, e^{(\sigma-\sigma_{no})/\sigma_1} ,$$

where σ is the applied tensile stress, $\dot{N}_o = 1 \times 10^{13}$ sec cm^{-3}, $\sigma_{no} = -3 \times 10^9$ dynes/cm^2 and $\sigma_1 = -9.5 \times 10^9$ dynes/cm^2.

A range of fragment velocities should be expected from the detonated warhead (BRL MR 2509, p. 18, 1975), and the given value of 3200 ft/sec (0.975 mm/μsec) falls within this range. A flat plate impact at this velocity will, according to the Hugoniot for iron, result in a compressive stress of 149 kbars.

$$U_{fs} = 0.975 \text{ mm/μsec.}$$

$$u_p = (1/2)\, U_{fs} = 0.488 \text{ mm/μsec.}$$

$$u_s = 2.049 + 3.79\, u_p = 3.899 \text{ mm/μsec.}$$

$$P = \rho\, u_p\, u_s = 149 \text{ kbars.}$$

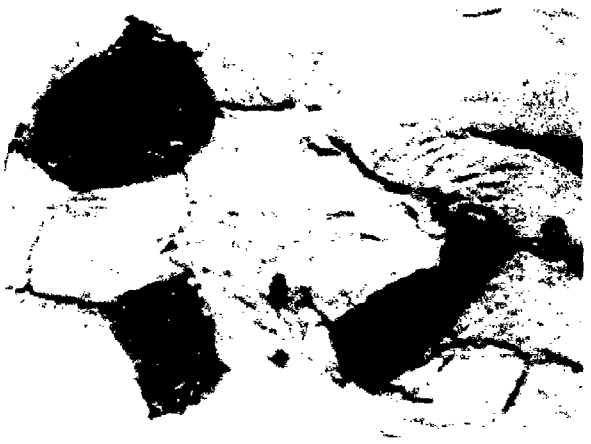

Figure A-1.

X 1500
Nital Etch
View along shell axis

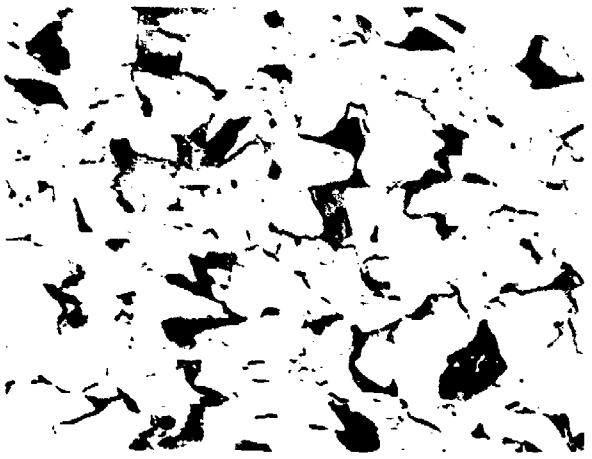

Figure A-2.

X 500
Nital Etch
View along shell axis

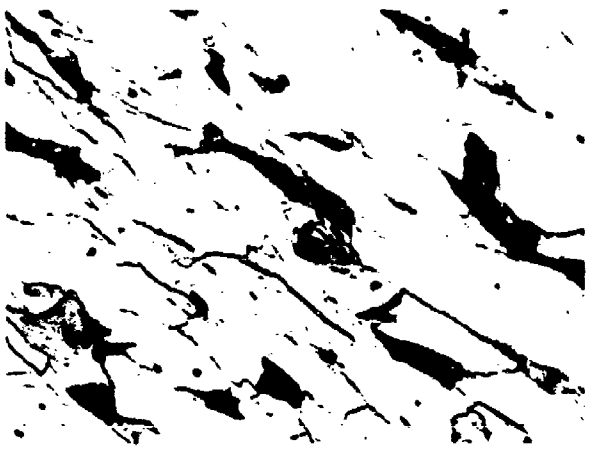

Figure A-3.

X 500
Nital Etch
View of radial section

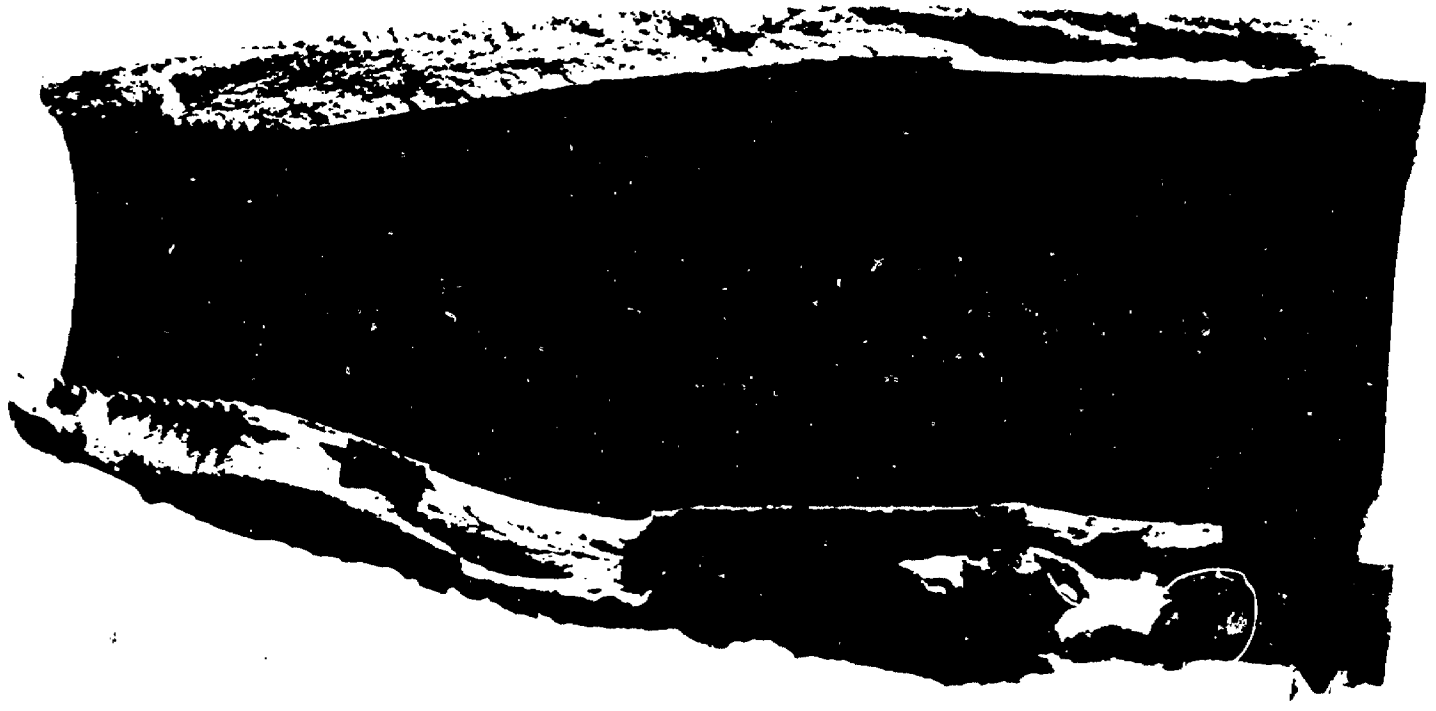

Figure A-4. Photograph of Inert Loaded 105mm HE Shell Subjected to Detonation of Another 105mm HE Shell 12 cm away

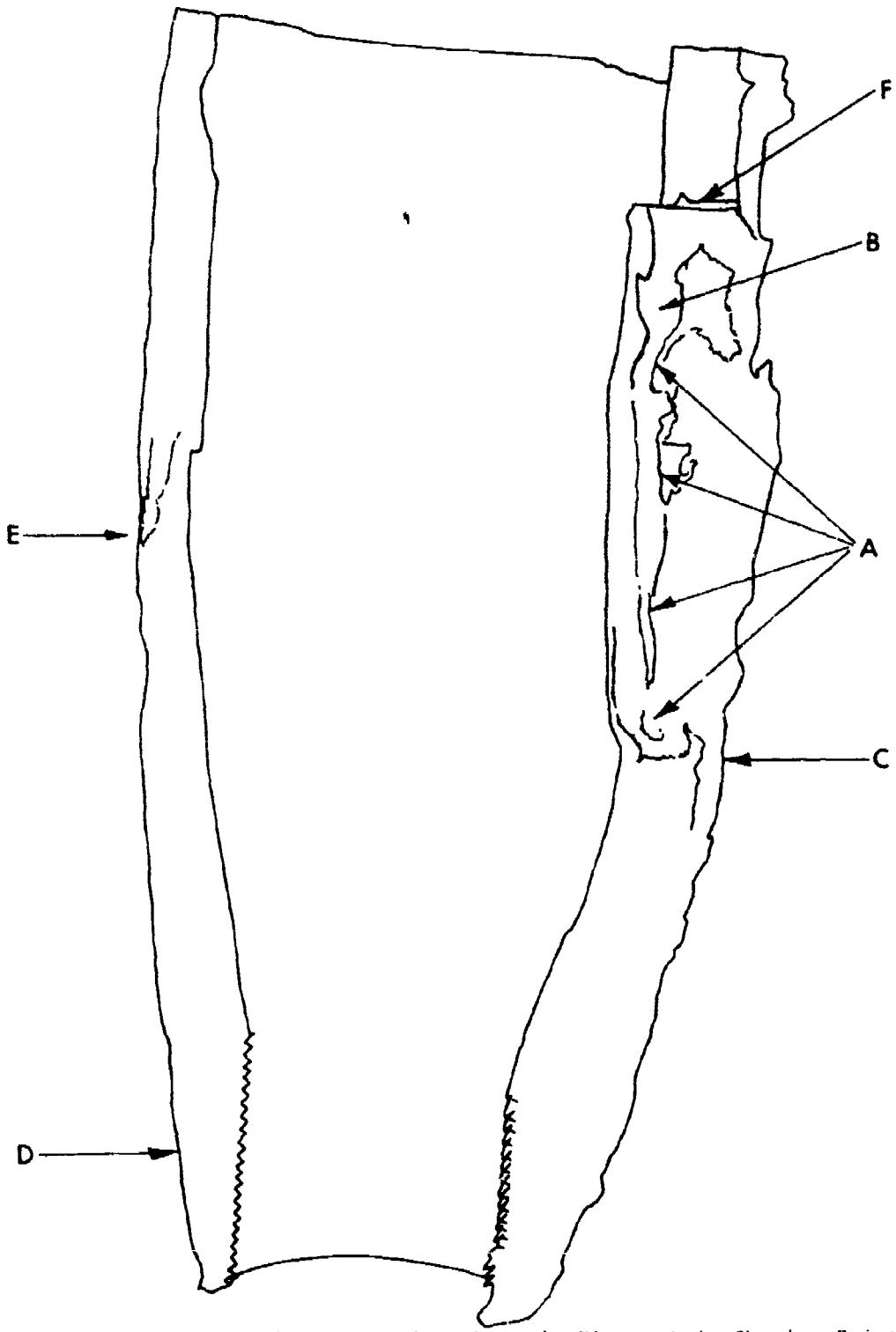

Figure A5. Schematic of Shell Casing shown in Figure A-4, Showing Points of Interest Discussed in Text

A net tensile stress of almost this magnitude will result later by stress wave reflections. This stress level is substantially greater than the threshold nucleation stress for void formation in ferrite which is only 3 kbars, and it is reasonable, therefore, to assume that spallation occurred in the impacted projectile even though the impact was not of flat parallel plates.

The line of intersection of the "V-notch" fracture, located approximately halfway between the inner and outer surfaces of projectile and between the locations A and B (Figures A-4 and A-5), is within the region where spallation should occur when there is an impact of plates of equal thickness.

The "V-notch" between locations A and B, the impact conditions and the nature of the material suggests that spallation should have occurred in a region bounding the midplane of the shell wall. The projectile was sectioned to check on the occurrence of spallation and to remove the confusion stemming from the unusually smooth and extensive exposed fracture surfaces at B (Figure A-5). The section observed (Location F, Figure A-5) was perpendicular to the projectile axis and is shown in Figure A-6. The tremendous number of microcracks within the specimen clearly verifies that there was substantial spallation.

It is proposed that the large shear surfaces resulted from the extensive inward structural bending due to the impact and the existence of the micropores left by the partial spallation. The stress field in the vicinity of a pore from this type of loading should be analogous to the stress field about a cylindrical cavity in a tensile specimen. Lines of constant shear stress in the plastic zone emanating from such a void are shown in Figure A-7 where it is shown that these lines intersect the void surface at 45 degrees, and at the top of the sample, the shear lines are also at 45 degrees to the direction of elongation. To verify that the shell wall was elongated by the impact, the wall thicknesses of the deformed shell were compared with those of an undeformed shell. The wall thickness measurements of the deformed projectile were made adjacent to both sides of the fracture on the impact side of the projectile. These measurements are listed in Table A-1 where it can be seen that almost all values of $(t_o - t_f)$ are positive, consistent with the proposed shear fracture model. It can be assumed, therefore, that the structural bending from the impact led to deformation and, thereby, stress concentions about the internal voids left from the earlier partial spallation. The voids from the spallation acted as fracture nuclei from which shear emanated and resulted in the planes of total separation at approximately 45 degrees to the shell wall. It is evident that it was the extensive shear that masked the micropores of the spallation by void coalescence on the shear planes. Evidence of this can be seen in Figure A-6.

From Point C (Figure A-5) to the tip of the shell, there is a river pattern (Figure A-8) to the fracture surface and shear lips at the inner and outer surfaces of the shell. The river pattern feathers outward

Figure A-6. Photomicrograph of Impacted Shell Casing Showing Incipient Spall

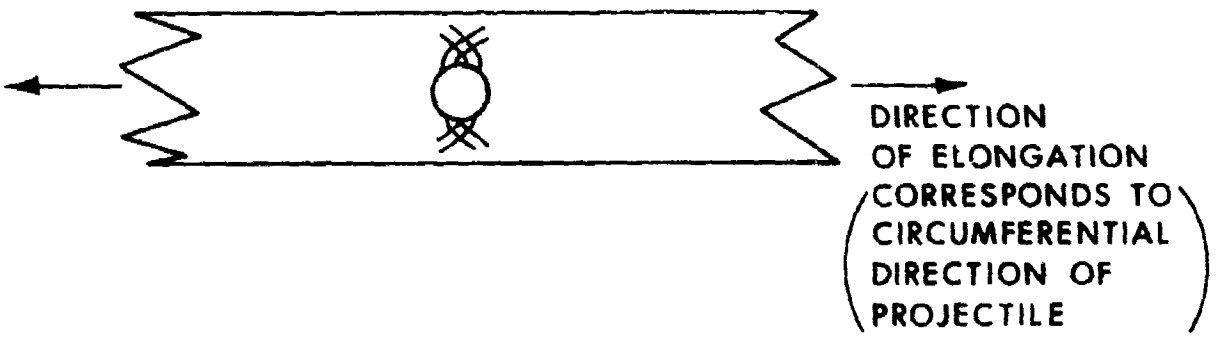

Figure A7. Schematic of Lines of Constant Shear Stress

Table A-1. Deformation Measurements

Distance from Small End of Shell cm.	Thickness Wall (original) $(t_o)_1$ in.	Thickness Wall (broken) $(t_f)_1$ in.	$(t_o)_1 - (t_f)_1$ in.	Thickness Wall (original) $(t_o)_2$ in.	Thickness Wall (broken) (t_f) in.	$(t_o)_2 - (t_f)_2$ in.
1	0.301	0.288	+0.013	0.307	0.272	+0.035
2	0.401	0.386	+0.015	0.405	0.369	+0.036
3	0.493	0.477	+0.016	0.496	0.444	+0.052
4	0.529	0.527	+0.002	0.537	0.532	+0.005
5	0.510	0.509	+0.001	0.526	0.513	+0.013
6	0.489	0.490	-0.001	0.506	0.494	+0.012
7	0.467	0.469	-0.002	0.487	0.475	+0.012
8	0.448	0.442	+0.006	0.469	0.451	+0.018
9	0.431	0.428	+0.003	0.453	0.428	+0.025
10	0.420	0.419	+0.001	0.441	0.425	+0.016
11	0.412	0.410	+0.002	0.431	0.417	+0.014
12	0.406	0.405	+0.001	0.423	0.408	+0.015
13	0.401	0.396	+0.005	0.416	0.398	+0.018
14	0.399	0.392	+0.007	0.412	0.402	+0.010
15	0.398	0.394	+0.004	0.412	0.402	+0.010
16	0.398	0.392	+0.006	0.412	0.398	+0.014
17	0.398	0.393	+0.005	0.410	0.397	+0.013
18	0.406	0.406	0.000	0.418	0.402	+0.016
19	0.409	0.416	-0.007	0.430	0.410	+0.020

*Positive numbers correspond to a reduction in wall thickness.

a. TWO SEPARATE CRACKS ON SLIGHTLY DIFFERENT PLANES. (CROSS SECTIONAL VIEW OF CRACKING)

b. BEGINNING OF CRACK COALESCENCE. (CROSS SECTIONAL VIEW OF CRACKING)

c. RIDGE OF RIVER PATTERN (THREE-DIMENSIONAL VIEW OF FRACTURE SURFACE SHOWING TRACE ON CROSS SECTION AS IN VIEWS a & b)

Figure 35. Schematic of "River Pattern" Development

from the centerline of the section and indicates the fracture progressed from Point C to the tip of the round.

At Point D (Figure A-5), there is a ledge in the fracture surface, and the river pattern below and above this point is oppositely oriented. These factors indicate that Point D was a crack nucleation site.

From D to E (Figure A-5), there is a steadily increasing amount of shear at the inner surface of the shell, and at E the fibrous fracture surface completely changes orientation. The ridges of the river pattern reveal that the crack progressed from the nucleation site at D toward E.

The partial shear fracture midway between the main fractures were due to the location of the impact and the change in inertia of the sample with position, i.e., the inertia at P_2 was a resistance to the motion from the impact at P_1 (Figure A-9).

C. Chronological Development of The Main Fracture

The crack growth sequence is shown schematically in Figure A-10.

a. Partial spallation occurred first halfway through the shell wall under the plane of impact.

b. Shear followed by starting at the voids left by the spallation and led to separation of the entire cross section under the impact.

c. The crack propagated from the spall zone to the small end of the round.

d. Fracture nucleated at the small end of the round on the side opposite the impact.

e. On the side of the projectile opposite the impact, the crack propagated from the small to the large end of the round.

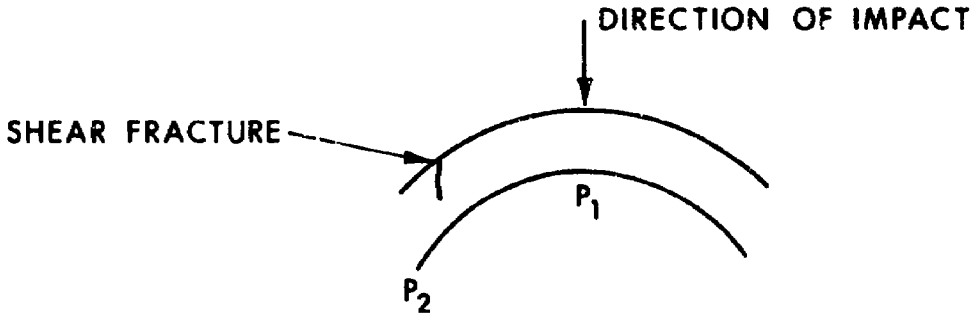

Figure A9. Schematic Showing Location of Shear Fracture Relative to Direction of Impact

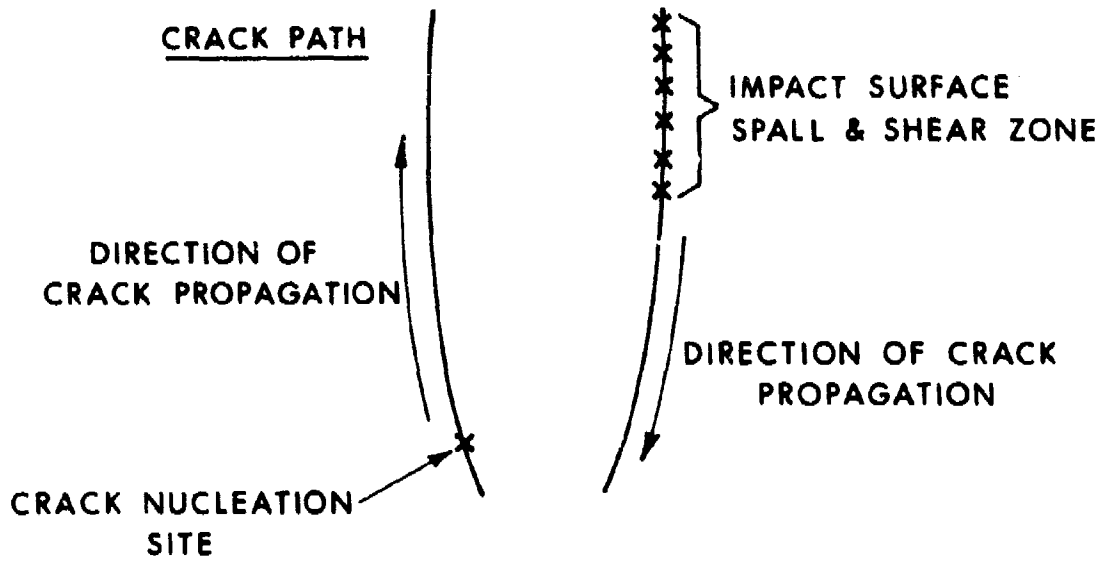

Figure A10. Schematic of Crack Growth Sequence

LIST OF SYMBOLS

P	pressure in shock wave
u	particle velocity in shock wave
U	shock velocity
t	time
ρ_o	unshocked explosive density
C	sound speed in shocked material
L	impacting projectile length
D	impacting projectile diameter
v	impact velocity of projectile
P_y	yield strength
σ_y	uniaxial tensile stress
d	diameter of test specimen
w	thickness of test specimen
h	thickness of acceptor warhead casing
r	radial deflection of target warheads
D	midsurface diameter in thin shell analysis
E	Young's modulus
i_o	impulse density
ν	Poisson's ratio
C_o	longitudinal wave speed
σ_c	uniaxial yield stress
V	fragment velocity
E	fragment kinetic energy/area
E^*	Gurney energy

LIST OF SYMBOLS

P	fragment momentum/area
M	mass of warhead casing
C	mass of explosive
R	distance from center of donor warhead to nearest surface of acceptor warhead
R_{50}	the value of R at which 50% of the acceptors detonate
R_o	radius of explosive charge
$\bar{V}$	average HE product velocity
r	radius of impacting projectile

SYMBOLS USED IN APPENDIX

$\dot{N}$	crack nucleation rate
$\dot{N}_o$	empirical constant
σ_{no}	empirical constant
σ_1	empirical constant
U_{fs}	free surface velocity
u_p	particle velocity
u_s	shock velocity
p	pressure behind shock
ρ	initial density